Pen-type electrodermal activity sensing system for stress detection based on likelihood ratios

by

Taehee Lee

B.S., Konkuk University, 2016

A THESIS

submitted in partial fulfillment of the requirements for the degree

MASTER OF SCIENCE

Department of Electrical & Computer Engineering
College of Engineering

KANSAS STATE UNIVERSITY
Manhattan, Kansas

2020

Approved by:

Major Professor
Dr. Steve Warren

Copyright

© Taehee Lee 2020.

Abstract

Psychological stress experienced during academic testing is known to be a significant performance factor for some students. While a student may be able to recognize and self-report stress experienced during an exam, unobtrusive tools to track stress in real time (and in association with specific test problems) are lacking. This effort pursued the design and initial assessment of an electrodermal activity (EDA) sensor - essentially a sweat sensor - mounted to a pen/pencil 'trainer:' a holder into which a pen/pencil is inserted that can help a person learn how to properly grip a writing instrument. This small assembly was held in the hand of a given subject during early human subject experiments and can be used for follow-on, mock test-taking scenarios. Data were acquired with this handheld device for 37 subjects (Kansas State University Internal Review Board Protocol #9864) while they each viewed approximately 30 minutes of emotion-evoking videos. Data collected by the EDA sensor were processed with an EDA signal processing app, which calculated and stored parameters associated with significant phasic EDA peaks. These peak data were then evaluated by a hypothesis driven stress-detection test that employed an approach using likelihood ratios for the ‘relaxed’ and ‘stressed’ groups. For these initial, motion-free testing scenarios, this pen-type EDA sensing system was able to discern which phasic responses were associated with ‘relaxed’ versus ‘stressed’ responses with 85% accuracy, where subject self-assessments of perceived stress levels were used to establish ground truth.

Table of Contents

List of Figures

List of Tables

Acknowledgements

I wish to express my deepest gratitude to my major professor, Dr. Steve Warren, who guided and encouraged me to be professional and achieve my academic goals. Without his help, this research project would not have been finished.

I also would like to offer special regards to my committee members, Dr. Bala Natarajan and Dr. Dave Thompson, for their insightful comments and suggestions.

I thank Dr. Don Gruenbacher and the Department of Electrical & Computer Engineering at Kansas State University for providing a superb learning, teaching, and research opportunity.

Lastly, I express my wholehearted appreciation to my mother, who supports me and encourages me to achieve my long-cherished dreams.

Chapter 1 - Introduction

Academic stress caused by test anxiety in classrooms is a significant factor that inhibits academic performance. Students who experience extreme test anxiety often obtain lower scores than they would have likely otherwise achieved. Detecting and analyzing student anxiety within an academic environment, especially during test-taking scenarios, by using unique pen-type electrodermal activity (EDA) sensors, could give educators insights into improving numerous facets of the educational system.

Methods to quantify anxiety/stress fall primarily into two categories: 1) electrochemistry methods such as cyclic voltammetry, which detects levels of the stress hormone, cortisol (present in blood or saliva) that are directly proportional to psychological stress [1], and 2) electrode-based sensing methods that employ electrocardiographs, electroencephalographs, and electrodermal activity circuitry to acquire biosignals mediated by the sympathetic nervous system [2, 3]. In this chapter, the motivation for work related to a pen-type EDA sensing system is addressed. Recent hormone-based psychological stress detection research is reviewed, and electrode-based stress monitoring systems are compared to systems that apply hormone-based methods. Finally, the benefits of a novel, pen-type EDA sensor are addressed in terms of overcoming challenges experienced by traditional hormone- and electrode-based approaches.

A. Research Motivation and Significance

A.1 Recent Stress Hormone Sensing Techniques and Their Disadvantages

The ‘stress’ hormone, cortisol, can be obtained from different types of biological samples, such as urine [4], interstitial fluid [5], hair [6], sweat [7], blood [8] and saliva [9]. Analysis methods that employ these body samples require devices that implement electrochemistry techniques, such as cyclic voltammetry [10], that can sense nanoscale

molecules. Another technique that can sense cortisol employs an immunoassay system [11], which requires ‘wet lab’ equipment that operates within a sterile environment to protect the samples from contamination.

Physical systems that implement such techniques prove unwieldy for typical academic test-taking scenarios. For example, the acquisition of bodily fluid samples from a student during an exam would be impractical for obvious reasons, including the creation of interruptions that may compromise the student's performance. Additionally, practical fluidic sensors that provide real-time, continuous data have not yet become widely available

A.2 Recent Biosignal Sensing Techniques for Stress Detection

A number of research efforts have used electrode-based biosignal sensing systems to detect and monitor emotions, especially stress. Biosignals and biological parameters that researchers study include electroencephalograms, electrooculograms, electrocardiograms, skin temperature, electrodermal activity (EDA), electromyograms, heart rate, heart rate variability, and respiration rate [12, 13] [14] [15]. Usually, to cross-validate these data and increase system sensitivity, researchers simultaneously acquire multiple signals and parameters. For example, S. Sriramprakash et al. monitored heart rate, heart rate variability, EDA, and electrocardiographic activity to detect stress in working people [2]. Another example is the wearable research conducted by F. Seoane et al., who used EDA, body temperature, electrocardiographic activity, electrical bioimpedance, and voice recordings in aggregate to assess mental stress [16].

Electrode-based biosignal measurement has advantages. It is relatively easy to make portable devices that measure these biosignals, and monitoring data in realtime is straightforward with the use of a single-board computer and a wired or wireless connection.

A.3 A Novel Pen-Type EDA Sensor

A typical EDA setup employs electrodes directly attached to the fingers - an arrangement that can hinder a student's ability to move and to manage the test materials in a natural way, potentially compromising their academic performance. It therefore seemed sensible to avoid this problem by developing a more novel EDA sensing approach. To that end, this work focused on the development and testing of a novel “pen-type” EDA sensor and the affiliated signal processing app and emotion-identification algorithms. The goal is to acquire anxiety-related biosignal data comparable with data presented in the prior literature without unduly affecting the ability of a student to perform on a written exam. Unlike a traditional arrangement, the electrodes of the pen-type EDA sensor are in contact with a subject’s index finger and thumb, which are usually the main fingers employed when writing with a pen or pencil. This is accomplished by the addition of a sleeve-like pen trainer into which a pen or pencil is inserted. This trainer, which also hosts the electrodes, will be described later in this document. Using this approach, a subject is freely able to utilize or put down the writing tool without undue interference from sensors and wiring. This flexibility enables the user to participate in additional activities, unlike traditional arrangements, where a subject is tethered to the measurement system.

A.4 Challenges for a Pen-Type EDA Sensor

This pen-type EDA sensing method does face technical challenges. For example, since the sensors are mounted onto a writing tool that holds a pen or pencil, motion artifacts will corrupt the EDA signals that the sensor acquires. It is not yet clear whether this motion artifact will be primarily additive, meaning that clever filtering will allow signal/artifact separation. If such motion artifacts can be removed, or at least minimized, in order to isolate relatively clean EDA data, then the pen-type EDA sensor will be employable in more practical testing

environments. Note that the studies employed here form a proof-of-concept investigation, so motion artifacts are intentionally avoided as part of the human subject testing described later in this document.

A.5 Significance of Monitoring Emotions During Academic Testing

In academic learning and testing scenarios, students experience a number of emotions and have varied emotional responses to certain academic tasks, especially test-related tasks. These emotional responses can have significant impacts on student achievement related to learning outcomes and course grades. It is therefore important to (1) understand the types of emotions involved in learning and test-taking and (2) be able to quantify individual emotional responses to these activities.

Psychological responses to educational environments include class-related, learning-related, and test-related emotions [17]. Well-known academic emotions are enjoyment, hope, pride, boredom, anger, anxiety, hopelessness, shame, and sadness [18] [19]. In the work presented here, some of these emotions will be addressed using pre-experimental survey questions. The intent is to understand the emotions that the subjects most associate with test-taking scenarios, with a goal to ascertain whether the pen-type EDA system developed for this effort can differentiate between these types of emotions as elicited by video media.

A.6 Research Purpose and Contents of Upcoming Chapters

The purpose of this effort is to assess the suitability of a lightweight, pen-type EDA sensing device to acquire stress-related data during an academic test-taking scenario – data that can be meaningfully interpreted in light of the existing EDA literature. Such a device would prove useful to continually assess exam-related stress without compromising the ability of a student to perform. This overall study will consist of two phases: 1) a phase to establish the early

viability of the pen-type sensor as a data gathering tool, where the device will be held by a given subject while they view emotion-evoking videos, and 2) a phase to assess the stress-detecting ability of the tool and its supporting software. Neither phase will yet address motion artifact, which has the potential to pose a substantial technical challenge.

In Chapter 2, basic EDA principles and terminology are explained based on skin anatomy and a related electrical model. In Chapter 3, research materials, procedures, data, and stress-detection approaches are summarized at a high level. Chapter 4 presents the prototype EDA device design and data acquisition method, then Chapter 5 addresses the signal processing approach applied to the EDA raw data. In Chapter 6, the purpose and significance of the pre- and in-experiment surveys are discussed as well as the content of the emotion-evoking videos used for these experiments. Chapter 7 presents experimental results, and Chapter 8 explains the stress-detection methods and results. Finally, Chapter 9 contains a summary of the research and suggests future work. Appendices A through F present the informed-consent form, the experiment survey sheets, the experimental protocol, selected experimental data, extra likelihood ratios for stress detection, and the PCB circuit design.

Chapter 2 - Electrodermal Activity

Sweat gland activity is controlled by sympathetic nerve activity [20], and the electrical properties of skin and its sweat glands play a role in this process. In this chapter, the principle behind electrodermal activity (EDA) will be discussed, and the corresponding model for the electrical properties of skin will be introduced, including the related terminology, electrical parameters, and units.

A. Principles of EDA Phenomena

A.1 Skin Anatomy

The schematic diagram in Figure 1 illustrates a vertical cross-section of the skin that contains an eccrine sweat gland and an apocrine sweat gland. The upper (outer) layer of the skin is called the epidermis, which consists of the stratum corneum, the stratum lucidum, a granular layer, a prickle cell layer, and a germinating layer [21]. The outer surface of the stratum corneum contains dead skin cells, under which living cells reside. The role of the corneum is to manage moisture by holding water on either the outside or the inside of the skin, then allowing that water to pass through the skin when necessary [22]. Usually, this layer of the skin is moderately hydrated, but the level of hydration (and therefore the skin resistance) varies depending on humidity changes in the external environment or by sweating. The eccrine sweat gland duct is comprised of a tube-like tissue made of epithelial cells, and it is re-absorptive with regard to sweat [23]. The palm offers the highest density of eccrine sweat glands, followed by the head. Eccrine sweat glands are ‘innervated’ by the sympathetic nervous system via cholinergic fibers. This type of sweat gland produces odorless, water-like sweat [24]. Unlike an eccrine sweat gland, an apocrine sweat gland secretes fatty sweat, and this type of sweat has an odor [25].

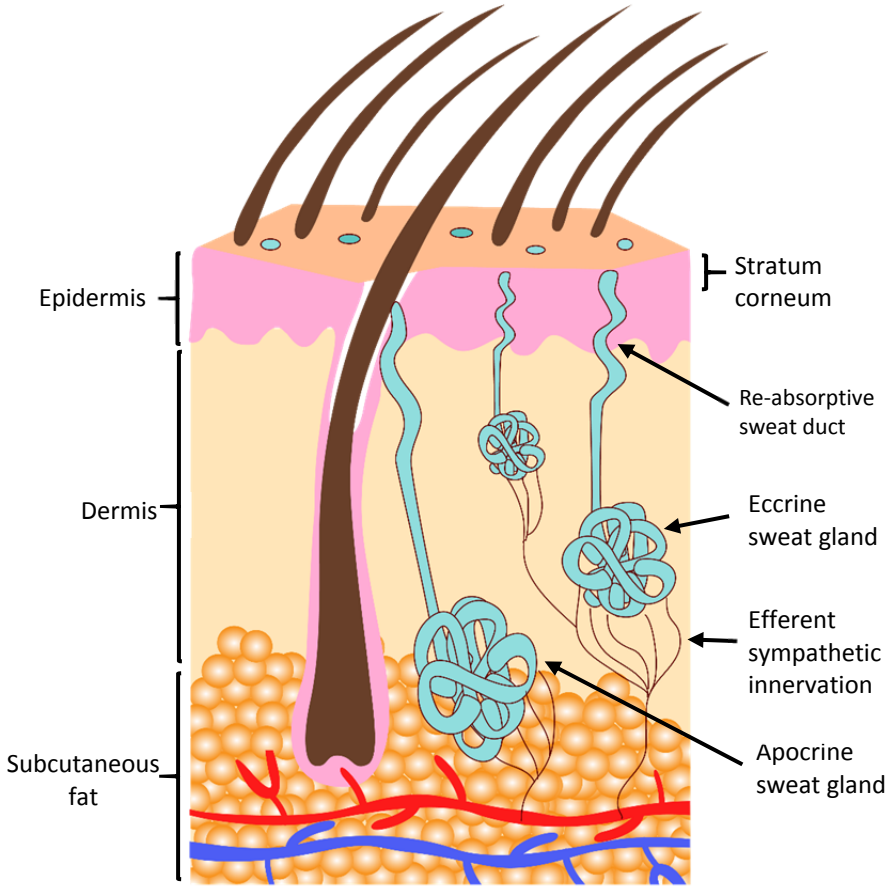

Figure 1. Schematic cross-section of the skin and a representative sweat gland.

A.2 Nervous System and Sweating

The central nervous system (CNS) controls body temperature via the hypothalamus, which is a small region in the center of the brain. The CNS sends signals to the autonomic nervous system (ANS), which regulates sweat glands via cholinergic fibers in the sympathetic nervous system (SNS) [20]. The CNS responds to changes in emotion as well, resulting in changes in sweat gland secretion that then affect skin electrical resistance [26]. As an example of emotion-induced sweating, some individuals' palms sweat when they feel nervous. Thus, using skin resistance, or skin conductance, as an emotion indicator is reasonable, and this measurement can be made with electrodermal activity sensors.

A.3 Electrical Properties of Skin and Sweat Glands: Resistive Model

When an external current is applied to skin, skin acts as an electrical component comprised of resistors and capacitors. For example, bio-fluids such as blood and sweat act as variable resistors, whereas cell membranes exhibit more capacitive behavior because these membranes are semi-permeable and hinder cross-membrane ion flow, resulting in ionic 'potentials' that exist across these cell membranes.

A resistive skin model [27] assumes that all skin components act like electrical resistors. Figure 2 depicts an example of a resistive skin model. Here, the stratum corneum acts like a variable resistor, whereas the epidermal barrier acts like a fixed resistor. The sweat gland ducts, which are switched on and off to be part of the circuit, act like electrical 'shunts' due to their low resistance [28].

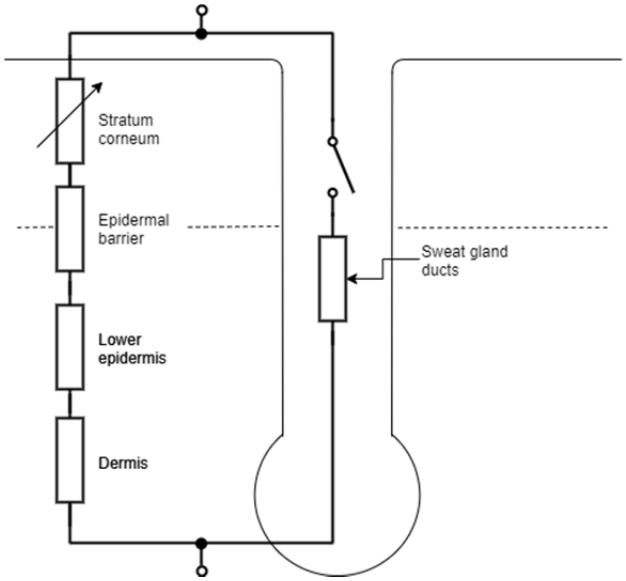

Figure 2. Schematic of a resistive model consisting of the skin and the sweat gland ducts.

When a sweat gland duct is switched 'on' to be part of the circuit, electrical current also flows through the duct in addition to the rest of skin layers. This occurs when the duct is filled with the sweat secreted from the gland after cholinergic innervation is applied [29]. The lower epidermis and the dermis have relatively low resistance, and their resistance is fixed, unlike the stratum corneum [30].

B. Terminology and Definitions

Electrodermal activity (EDA) is a term that is used to represent electrical changes in skin properties. The term 'galvanic skin response' is no longer recommended for use because of its improper implication that the skin is a galvanic element [27, 31]. Of all of the parameters associated with EDA, skin conductance has been the most studied. Skin conductance can be measured by applying an electrical voltage across two skin locations, where the amount of current flowing between these two spots is commensurate with skin conductance.

Electrodermal activity (EDA) has two components: tonic and phasic, as noted Figure 3. Tonic EDA represents the skin conductance level (SCL), which has the character of a slowly changing baseline. Phasic EDA represents the skin conductance responses (SCRs) – temporal phenomena which reflect changes in sympathetic neuronal activity. Phasic EDA is either event-related or non-specific. Event-related, phasic EDA occurs in response to psychological stimuli, whereas non-specific, phasic EDA consists of naturally occurring phasic peaks without stimuli.

An electrodermal measurement technique that does not involve an external current is defined as endosomatic. In comparison, an exosomatic measurement approach utilizes either direct current (DC) or alternating current (AC). When the acquired voltage is kept constant during a DC measurement, EDA is reported with skin conductance (SC) units, whereas when the acquired current is kept constant, EDA is reported with skin resistance (SR) units. When the

acquired voltage is kept constant during an AC measurement, EDA is reported with skin admittance (SY) units, whereas when the acquired current is kept constant, EDA is reported with skin impedance (SZ) units [32].

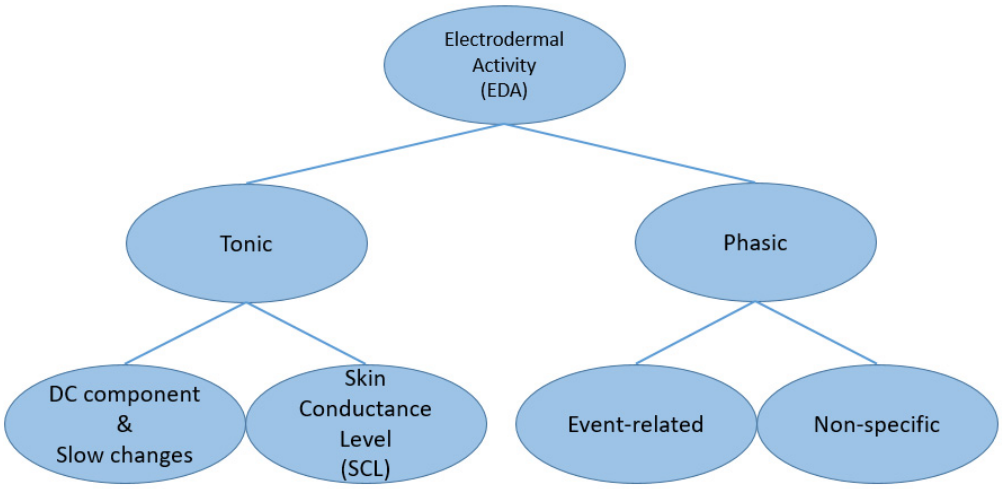

Figure 3. Components of electrodermal activity.

C. Units

Electrodermal activity is reported using the SI unit of Siemens (S). The electrical conductance of a component, G, is defined as

$$G = \frac{1}{R} = \frac{I}{V},$$

where R is the electrical resistance, V is the voltage across the component with a conductivity, G, and I is the current flowing through the object. The electrical conductance, G, is reported in Siemens (S):

$$\mathrm{S} = \Omega^{-1} = \frac{A}{V},$$

where A is amperes and V is volts.

D. EDA Signal Parameters

EDA signal parameters can be visually explained using the prototypical EDA signal depicted in Figure 4. In a case of an event-related EDA signal (a signal caused by a physiological stimulus), the EDA signal level rises after a short period of latency. In contrast, a non-specific phasic EDA signal (a signal not caused by a particular physiological stimulus) occurs with a frequency of 1-3 peaks/min [33]. Once the EDA signal reaches its peak, the signal starts to decrease, reaching 50% of its peak amplitude at the 'half-recovery' time, followed by 63% of its peak amplitude at the 'recovery time.' Parameter descriptions related to Figure 4 follow:

- **Latency**: the time period between the stimulus and the onset of the phasic response.
- **Response onset time**: the time when the SCR rises from the base skin conductance.
- **Rise time**: the time difference between the EDA signal onset time and the SCR peak.
- **Half recovery time or decay time**: the time period between the SCR peak and 50% of amplitude.
- **Recovery time**: the time period between the SCR peak and 63% of amplitude.
- **Response peak**: the highest point of a single EDA response window after a stimulus is applied.
- **Amplitude**: the difference between the response peak and the baseline.

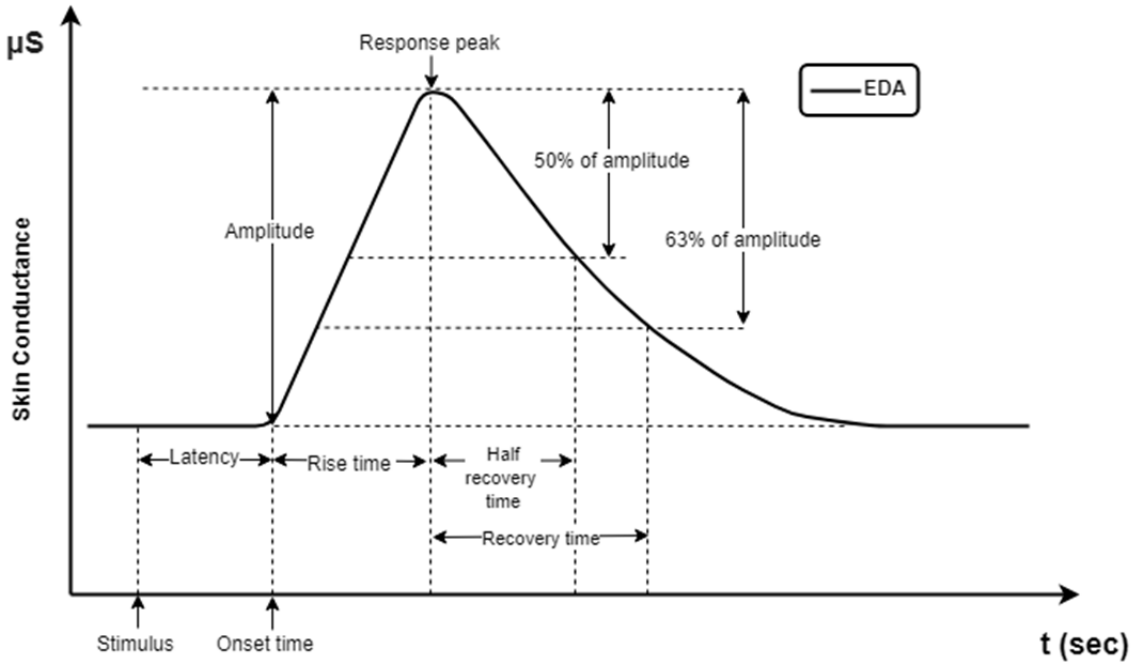

Figure 4. Prototypical electrodermal activity signal.

Chapter 3 - Research Methods

In this chapter, the research materials, procedures, data-management processes, and stress-detection methods will be addressed in detail. The *Materials* section addresses items incorporated into the sensing unit, a basic introduction to the emotion-evoking video content used during the experiments, and pre-and-in-experiment surveys offered to the participants. The *Procedures* section speaks to subject recruitment and the experimental procedure. Next, the *Research Data Management* section focuses on the signal processing method and the experimental results. Finally, the *Stress Detection* section briefly addresses the methodology used to classify data sets into 'relaxed' versus 'stressed' categories.

A. Materials

A.1 Pen-Type Electrodermal Activity (EDA) Device

Figure 5 displays a picture of EDA electrodes mounted on a pen-type 'writing trainer'. The writing trainer, into which a pen or pencil is inserted, is used to teach a student how to properly hold a writing instrument by providing a stable and fixed grip platform. Such a hand grip is comfortable and does not compromise a person's handwriting ability or style. Various commercial ergonomic training grips can be found online, and the lightweight grip design, *MegaTrue Pencil Pen Ergonomics Handwriting Aid Grip for Adult and Kids* [34], has been chosen for this research. The prototype EDA sensing device incorporates a modified version of this writing trainer that employs two EDA electrodes made from copper tape – see Figure 5. These electrodes are attached to the grip at the contact locations for the thumb and index finger. The electrodes are connected to the sensing circuitry, which produces a differential analog, electrical-current signal that can be stored, analyzed, and interpreted to provide indicators for

psychological stress consistent with the EDA literature. Hardware component details and signal processing methods are discussed in Chapters 4 and 5, respectively.

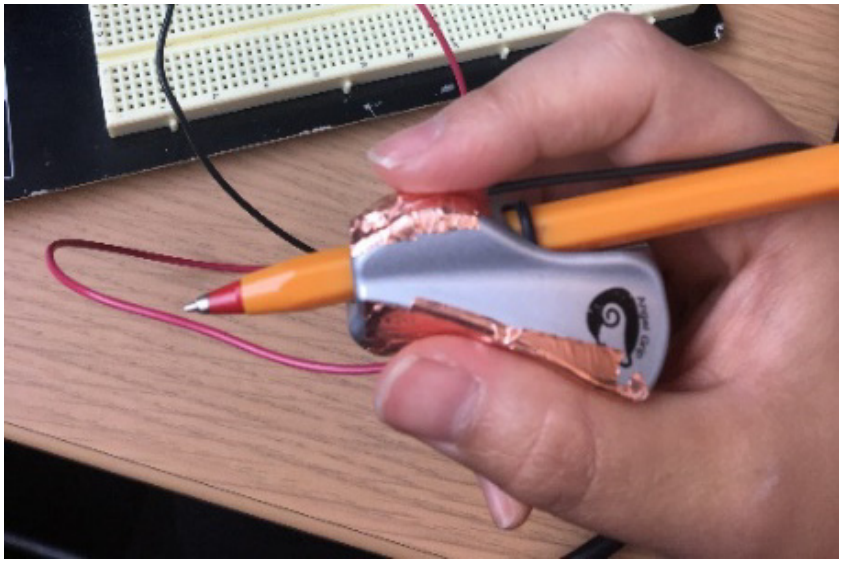

Figure 5. Pen-type EDA electrodes mounted on a writing trainer.

A.2 Experimental Video Content

The video series assembled for these early experimental analyses is approximately 30 minutes long and includes a comforting Mozart music playlist, an extreme parkour clip, a jump-scaring video, a video of a pet owner saying goodbye to his sick dog, and a video of near misses – see Chapter 6 for details. This material has been chosen to evoke emotions that may be representative of the emotions experienced during a test-taking scenario. The Mozart music was chosen to evoke relaxation; the extreme parkour clip was chosen to evoke anxiety; the jump-scaring video was chosen to induce both anxiety and surprise; the 'saying goodbye' video was chosen to evoke sadness or stress; and the near-misses video was chosen to induce anxiety or stress. None of this material was intended to evoke extreme emotions and therefore does not include any depictions of oppression, bullying, suicide/death, abuse/torture, or other extremely upsetting or graphic subject matter. Additionally, the material does not include any pornographic

content or other material that may be described as 'adult' in nature. The experimental videos, surveys, and protocols were reviewed and approved by the Kansas State University Institutional Review Board under protocol #9864.

A.3 Experimental Survey Content

The survey content employed in each experimental session had two components: 1) a pre-experiment survey and 2) an in-experiment survey – see Appendix B. The purpose of the pre-experiment survey was to investigate which positive and negative emotions the subject associates with the process of 'taking an academic exam' based on their past experiences. Analyses related to this survey component will offer insight into psycho-physiological reactions experienced in academic settings, especially during exams. According to Spangler et al., and Pekrun et al., academic exam-related emotions include pride, anxiety, hopelessness, anger, joy, boredom, shame, and hope [17] [35]. The pre-experiment questionnaire offered these specific emotions as responses, plus adds sadness. Once the subject chose the emotions that they associate with the process of taking an academic exam, they then rated each emotion on a scale of 1 to 10 in the context of a typical exam experience, where 1 is a minimal sense of emotion and 10 is an extreme sense of emotion. The ratings by the individual subject offer comparative tolerances for each emotion. For example, if the subject chose sadness and rated sadness at 8 out of 10, this subject would be considered to have a low tolerance related to sadness during academic exam settings, or possibly in non-academic settings as well.

Negative emotions that were included in the pre-experiment survey are categorized as 'emotional stressors' in this research. Out of all negative academic emotions, mainly sadness and anxiety/nervousness are triggered by the experimental videos. Likewise, out of all positive academic emotions, relaxation is primarily triggered by the experimental videos. There are

reasons why sadness, anxiety, and relaxation were emphasized by this research. First, sadness was chosen because academic failure brings about sadness, clearly implying that sadness can be a good indicator for academic stress [36]. Second, relaxation plays a role in the opposing emotions – anxiety or stress – which allows the researcher to quantitatively analyze stress or anxiety in comparison to relaxation. Third, anxiety is the main target for this research; it is the 'problem' emotion that most often hinders students from achieving good grades on academic exams. EDA signals arising from anxiety will be compared with those that arise from relaxation and sadness. Detailed information regarding these analyses and results can be found in Chapters 7 and 8.

B. Procedures

B.1 Experimental Procedure

At the beginning of each experimental session, the subject was asked to read and sign the informed consent form (see Appendix A). The subject then completed a short pre-experiment survey (see Appendix B) that begins with a self-assessment regarding the subject's perceived levels of emotion in academic environments, particularly test-taking scenarios. The researcher then asked the subject to hold the EDA sensing device so that the researcher could verify that the associated signals were within the active range of the data acquisition equipment. At that point, the subject then engaged in an ordered exposure to the image- and video-based material as laid out in the session protocol (see Appendix C). In between each pair of videos, the subject was asked to answer 'in-experiment survey' questions (see Appendix B), which addressed how much the prior video affected various subject emotions on a scale of 1 to 10. The entire session was videotaped as a means to both archive the process and to seek other physiological parameters that may serve as supplemental indicators of stress/anxiety.

B.2 Subjects and Subject Recruitment

Thirty-six individuals comprised the subject pool for this initial study and the affiliated analyses. Each of these individuals had experience as a student in a post-secondary academic environment, and each subject was between 18 and 35 years of age and was able to provide their own informed consent. These subjects were recruited via email, word of mouth, posted signage, and online advertisements. Korean subjects received informed consent forms, surveys, and debriefing statements that were translated into the Korean language.

C. Research Data Management

C.1 Subject and Data Protection

All electronic data (EDA signals, ECGs, videos, etc.) were stored on a password-protected network drive managed by the KSU College of Engineering and/or password-protected computers managed by the PI and the graduate student who conducted this work. Signed consent forms (see Appendix A) and any physical session materials were stored in a locked file cabinet. To maintain subject confidentiality, each participant was initially assigned a unique number that was thereafter used to identify them.

C.2 Signal Processing

All acquired EDA data were processed with a MATLAB-based app designed for this EDA research. The app can identify and store significant peaks along with other parameters such as amplitudes, peak times, onset times, and rise times. Detailed information about the EDA signal processing app can be found in Chapter 5.

C.3 Experimental Results

Resulting data, such as pre-experiment survey results, in-experiment survey results, and signal processing results, are summarized and discussed in Chapter 7. The pre-experiment survey results are displayed in the form of a table and a pie chart. In the pre-experiment survey result table, ratings related to each 'academic emotion' are enumerated and then converted into 'scores' used to create the pie chart. Similarly, enumerated in-experiment survey results, consisting of ratings related to each emotion-evoking video, are displayed in the form of table. Finally, the signal-processing results are collected and exhibited in the form of box plots. The signal-processing results involve several parameters such as phasic EDA amplitude, rise time, slope, and peak frequency. The box plots contain statistical information regarding the amplitude average, minimum, maximum, standard deviation, first quantile, third quantile, median, and skewness for each emotion evoking video. Moreover, given these phasic EDA amplitude results, a mean *t* test was conducted to verify that certain data sets are statistically different from each other, which validates the final step, which is 'stress detection,' as summarized in the next section.

D. Stress Detection

The goal for this phase of the research is to be able to determine whether a phasic response should be perceived as arising from a 'relaxed' versus a 'stressed' individual. After basic signal processing is performed to smooth the EDA signals and to extract parameter values, the data from all subjects are divided into either ground-truth data or non-ground-truth data for a given type of emotive response. Ground-truth data are data from subjects who indicated an in-experiment survey answer of 5 or above after watching a given video (e.g., the stressed individuals). Non-ground-truth data are from the subjects who indicated a survey answer smaller

than 5 (e.g., the relaxed individuals). After this separation process, only ground-truth data are chosen to evaluate the stress detection system. A chi-squared goodness-of-fit test is conducted with a portion of the ground-truth data to validate the 'training' model. Then, the 'test' data (the remaining portion of the ground-truth data) go through a likelihood ratio test to either accept or reject the null hypothesis (i.e., the test data belong to the 'relaxed' group), whereas the alternative hypothesis assumes that the test data belong to the 'stressed' group. More detailed information can be found in Chapter 8.

Chapter 4 - Prototype Design and Data Acquisition System

This chapter addresses prototyping, data acquisition, signal processing, and data analysis methods related to the EDA system. A block diagram of the pen-type EDA process is illustrated in Figure 6. This process can be divided into two phases: data collection and signal processing. The first phase relies on hardware functionality, including the electrodes, the printed circuit board which contains the lowpass filter, and the microcontroller sub-system that enables real-time data monitoring. The second phase includes the algorithm to extract the phasic EDA events from the raw EDA signals so that the system can identify significant phasic peaks, as well as their respective onsets and offsets, while excluding the tonic EDA elements that have little psychological meaning for stress detection. After detecting the significant phasic EDA peaks, the system categorizes the associated subject as relaxed or stressed based on a statistically established model.

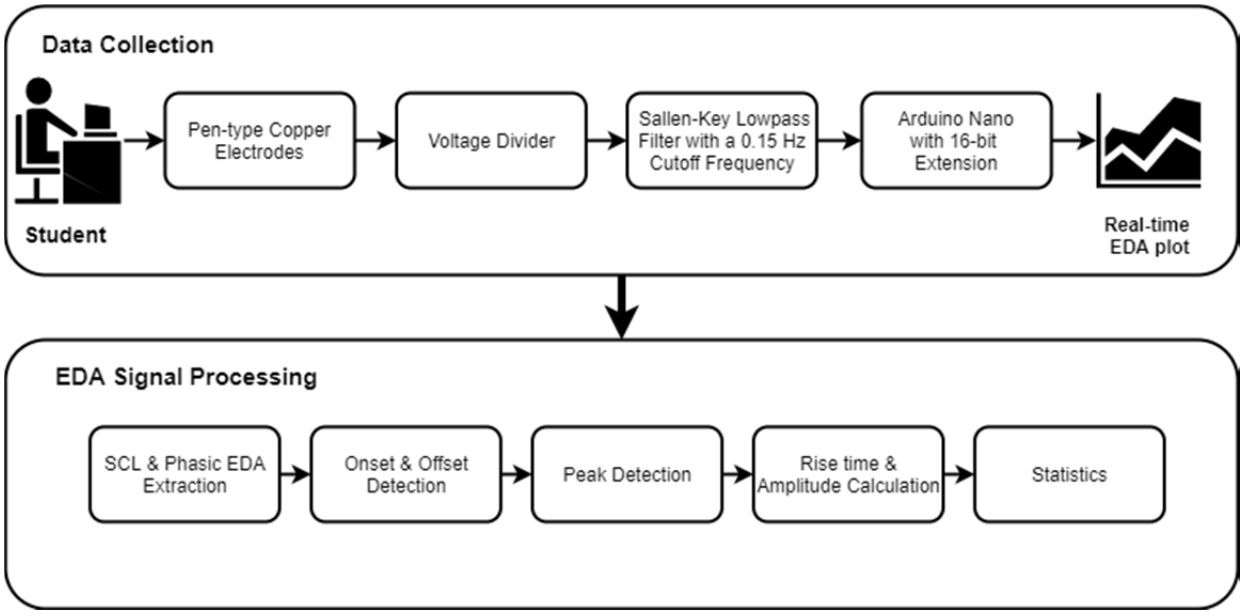

Figure 6. Block diagram – EDA data collection system and signal processing approach.

A. Hardware Design

The electrode-based sensing circuitry and the associated data acquisition hardware provide an electrical voltage output that can be mapped to skin conductance, which is then proportionally related to the perceived level of psychological stress, consistent with the EDA literature. This system includes an Arduino Nano microcontroller unit [37](with a 16-bit analog-to-digital converter (ADC) extension) that coordinates the analog circuitry and the conversion of analog signal data into digital data suitable for computer storage and analysis. When a person who holds this pen-type EDA monitoring system is nervous, their hand becomes sweatier, and the electrical resistance between their thumb and index finger decreases, allowing more current to flow between the respective electrodes, which are powered by a constant voltage. The prototype, which uses a 5 V power source, will produce electrical current amplitudes that range from approximately 5 μA to 15 μA, depending on the subject's level of anxiety, which corresponds to thumb-to-finger tissue resistances of approximately 1.25 MΩ to 5000 MΩ and skin conductances of approximately 0.0002 μS to 0.8 μS. This corresponds to current levels of 1 nA to 3.4 μA. Such a current will flow, e.g., from one electrode into the index finger, through a portion of the user's hand, and then out of their thumb and into the other electrode. These electrical current amplitudes are safe [38], the currents are imperceptible to the subject, they are limited only to the region of the hand between the electrodes, and they do not alter the subject's tissue in any way.

Figure 7 displays a picture of the EDA electrodes attached to the pen-grip trainer. The electrodes are constructed from conductive copper tape, which has been used for electrode material in other biomedical engineering research [39]. This handgrip form factor is natural and comfortable; it does not compromise the subject’s handwriting process or style. Further, the

electrodes offer excellent contact with a subject's thumb and index finger toward acquiring a good EDA signal, and the controlled handgrip offered by the trainer ensures subject-to-subject consistency in terms of electrode placement. The electrodes are soldered to wires that interface with the downstream circuitry, which is comprised of a voltage divider followed by an analog lowpass filter. An Arduino Nano is used as both a microcontroller and a power source, since it can supply 5 V via a USB connection to a computer. The Arduino Nano uses an Atmega328 8-bit AVR microcontroller [37]. To gain higher precision on the sampled data, an ADS1115 16-bit ADC [40] was used along with the Arduino Nano, which by default offers a 10-bit ADC. The MegunoLink software [41]was chosen for data storage and real-time plotting.

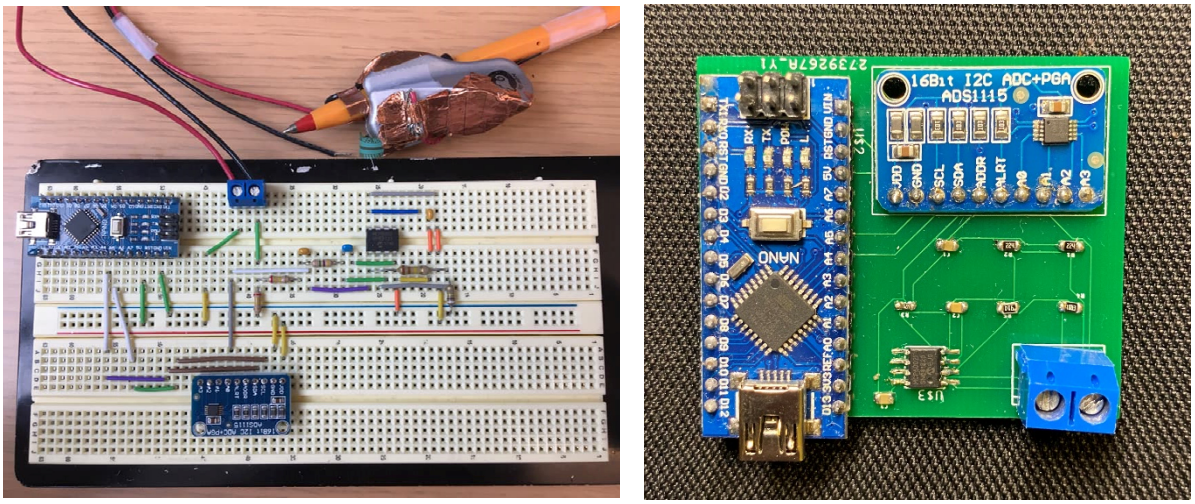

Figure 7. Pen-type EDA sensor prototype, with circuitry on a breadboard (left) versus a printed circuit board version of the hardware (right).

As depicted in Figure 8, other electronic devices are incorporated into the EDA data collection system: a video screen to display the emotion-evoking videos, Bluetooth headphones worn by the subject, and an EDA real-time monitor that the researcher can use to view data and initiate or pause data collection. The ground loop isolator is explained later in this chapter.

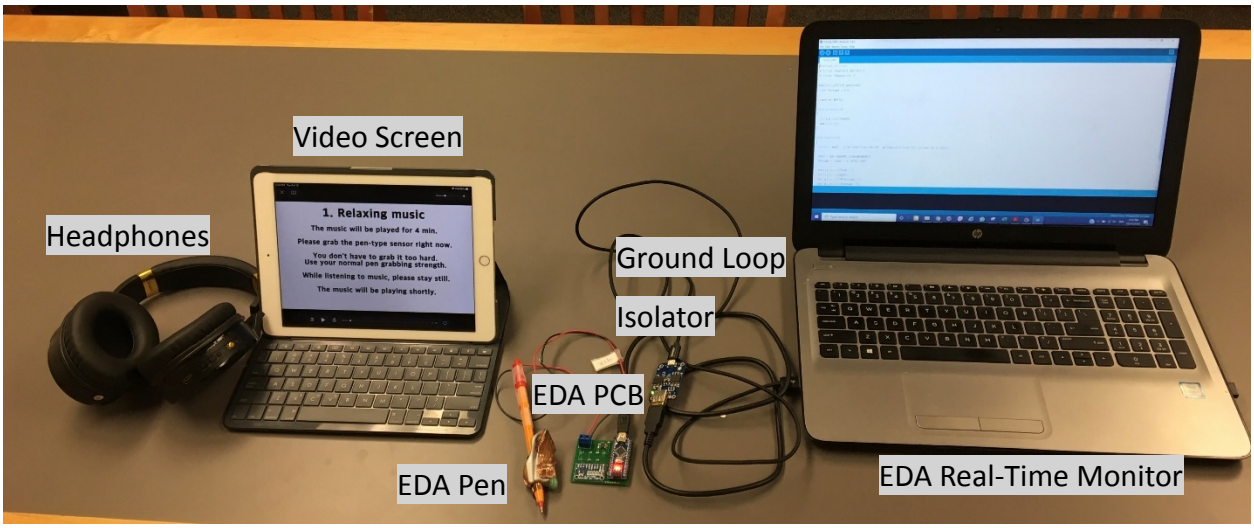

Figure 8. EDA data collection hardware.

Figure 9 contains a representative picture of an EDA data collection session. Data collection was performed in an isolated room with minimal likelihood for interruptions such as drop-in visitors, hallway noise, or visual distractions, any of which might lead to data corruption from unrelated psychological disturbances.

Figure 9. A representative EDA data collection session.

A.1 Voltage Divider

As mentioned above, the EDA sensing electrodes are connected to a downstream voltage divider whose voltage output varies as a function of R1, the skin resistance of the subject (see Figure 10). Given this arrangement, skin conductance in Siemens as a function of the measured output voltage can be calculated as below.

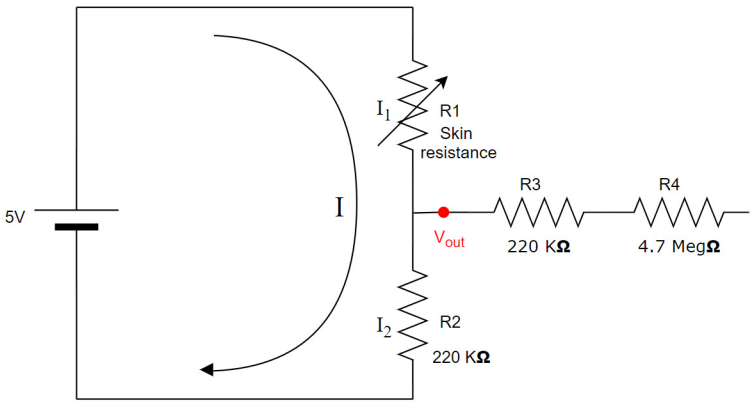

Figure 10. Voltage divider circuitry.

$$V_{out} = I \cdot R_2$$

$$I = \frac{V_{out}}{R_2} = \frac{V_{out}}{220\ K\Omega}$$

$$I = \frac{V_{out}}{220\ K\Omega}$$

$$R_1 = R_2 \cdot \left(\frac{V_{in}}{V_{out}} - 1\right) = 220\ K\Omega \cdot \left(\frac{5\ V}{V_{out}} - 1\right)$$

$$\text{Skin Conductance} = \frac{1}{R_1} = \frac{1}{220\ K\Omega \cdot \left(\frac{5\ V}{V_{out}} - 1\right)} = \frac{V_{out} \cdot 10^{-3}}{1100 - 220 \cdot V_{out}}\ \Omega^{-1}$$

$$= \frac{10^{-3}}{\frac{1100}{V_{out}} - 220}\ \Omega^{-1} = \frac{1}{\frac{1100}{V_{out}} - 220}\ \text{mS} = \frac{1000}{\frac{1100}{V_{out}} - 220}\ \mu\text{S}$$

A.2 Filter Design

A second-order, Sallen-Key lowpass filter with a cutoff frequency of 0.15 Hz (see Figure 11) was employed as a downstream filter to attenuate higher-frequency signal noise. This active filter is a form of a voltage-controlled voltage-source (VCVS) filter which has, for practical purposes, an 'infinite' input impedance and an output impedance of 'zero.' This means that the output voltage of the upstream voltage divider will not measurably drop at the filter input: the filter will not provide an appreciable load to the voltage divider. The important components of the EDA signal exist at relatively low frequencies ranging from ~0.045 Hz to ~0.25 Hz [42] [43], so the chosen cutoff frequency of 0.15 Hz will pass the signal components of interest along with their respective harmonics. In support of this point, Figure 12 displays a magnitude spectrum for a representative EDA signal, where the spectral coefficients include a rather large DC baseline and smaller-magnitude coefficients confined to a frequency range of approximately [0, 0.1] Hz.

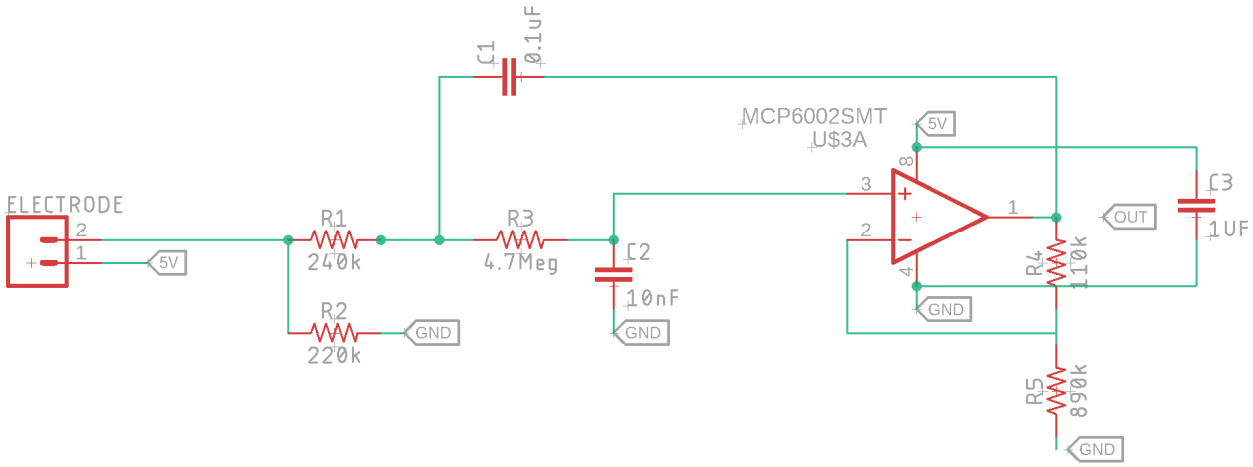

Figure 11. Sallen-key lowpass filter employed in the EDA detection system.

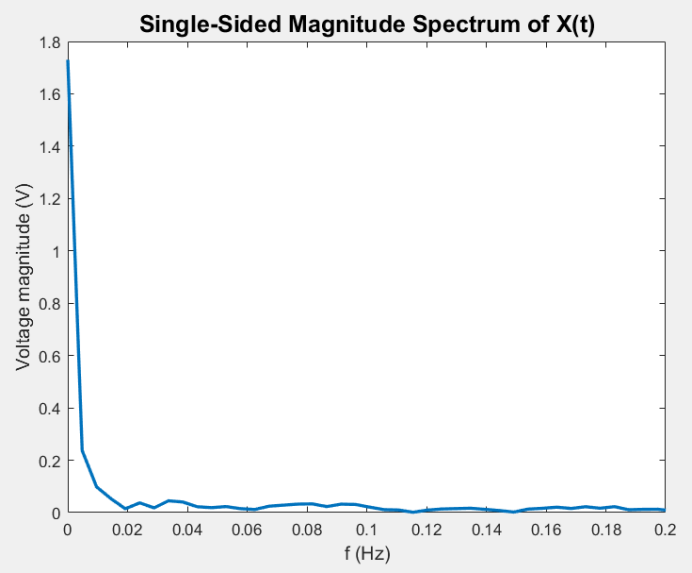

Figure 12. Typical single-sided magnitude spectrum for sampled EDA data.

A.3 Electrical Isolation

For safety purposes, a commercial electrical isolation unit (Adafruit USB isolator [44], also referred to as a ground-loop elimination unit – see Figure 13) was incorporated into the EDA sensing system. This unit offers electrical isolation for both the power source and the detected signal, meaning that the subject will never become part of an electrical current path to ground. The circuit schematic for this PCB unit is displayed in Appendix F [44].

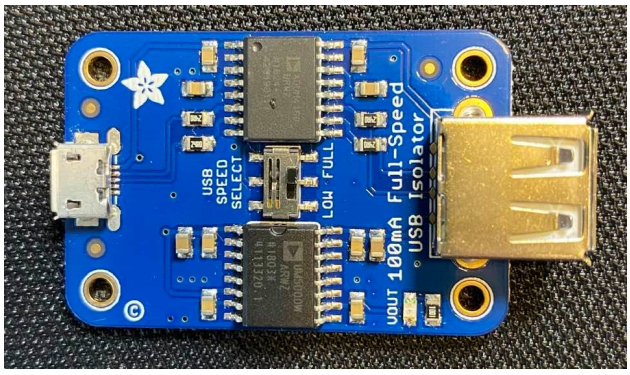

Figure 13. Adafruit USB isolator.

A.4 EDA Electrode Contact Sites

Conventional palmar EDA electrode sites are located at areas 1, 2, 3, and 4, as illustrated in Figure 14. For this pen-type EDA sensor platform, it is more convenient to use the thumb and index finger (areas A and B in Figure 14) as electrode contact sites, because the hand-grip trainer offers consistent access to these points given the natural grip arrangement that the trainer promotes. Early studies confirmed that contact points A and B yield sensible EDA signals.

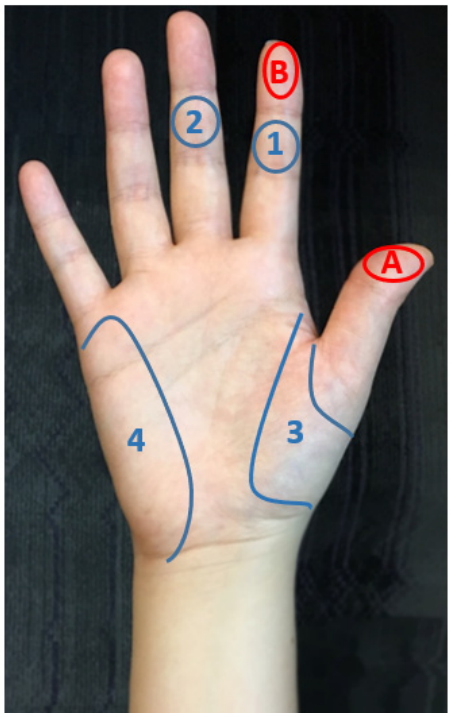

Figure 14. Palmar electrode sites.

Chapter 5 - EDA Signal Processing

A. Signal Processing App

Processing of these EDA data is needed prior to further data storage and analysis. Raw data collected via the MegunoLink software are stored in a `.csv` file format. These raw data are fed into an EDA signal processing app developed with the MATLAB App Designer [45] – see the graphical user interface depicted in Figure 15. Three parameters (slope threshold, peak distance threshold, and phasic extraction average filter window size – displayed on the right side of Figure 15) control the signal processing sequence, and various parameters are reported for each individual raw data set (e.g., note the parameters in the lower right corner of Figure 15). Parameters affiliated with the signal processing approach are defined in the next section.

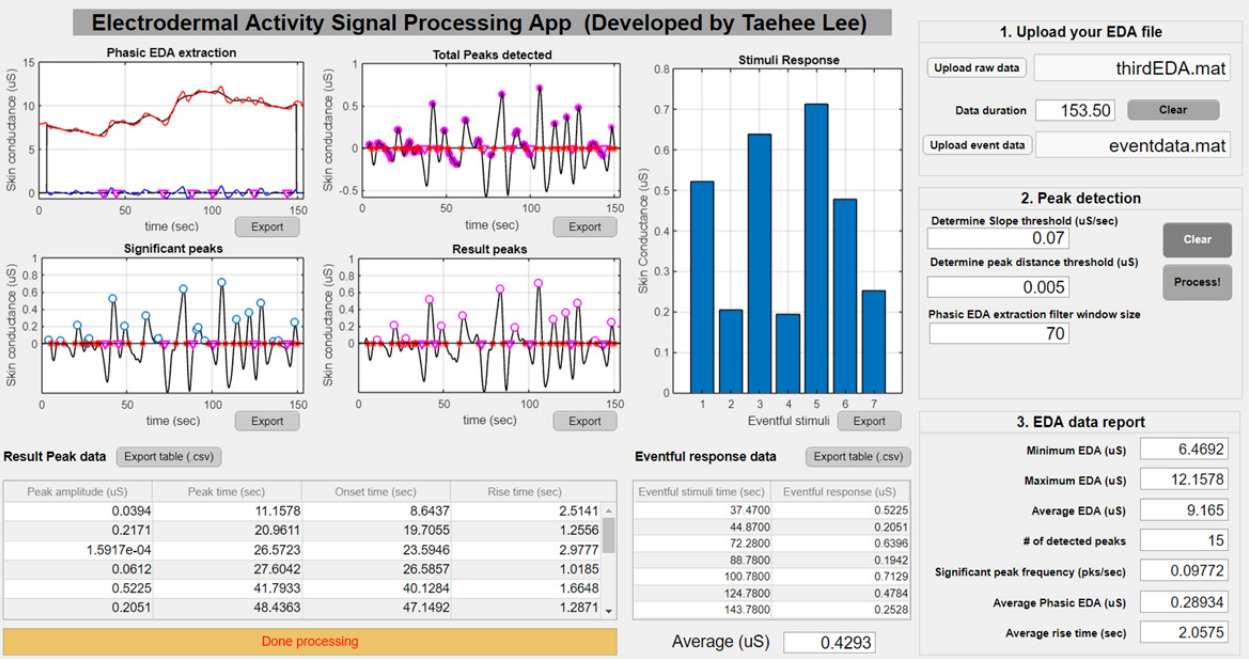

Figure 15. Electrodermal activity signal processing app graphical user interface.

A.1 App Input Parameters

Parameters that act as inputs for the signal processing app follow:

- **Slope Threshold (µS/sec)**: the slope value that is close to zero and helps to determine whether the EDA signal, $EDA\ (S_n)$, has a possible peak at the data point, S_n, by comparing $\Delta Phasic_{EDA}\ (S_n)\ /\Delta S_n$ with the slope threshold. The ideal slope threshold is zero, at which point the EDA signal has an inflection. However, it is unlikely that the discrete $Phasic_{EDA}\ (S_n)$ has $\Delta Phasic_{EDA}\ (S_n)\ /\Delta S_n$ of exactly 0 at a point of inflection. Thus, if $\Delta Phasic_{EDA}\ (S_n)\ /\Delta S_n$ is smaller than the slope threshold, the selected S_n are considered to have a point of inflection among them.
- **Peak Distance Threshold (µS)**: the threshold that determines whether multiple S_n data points are detected around one point of inflection of the EDA signal, by comparing the distance between $Phasic_{EDA}\ (S_n)$ and $Phasic_{EDA}\ (S_{n-1})$ with the distance threshold.
- **Phasic EDA Extraction Filter Window Size**: The moving average filter size used to extract phasic EDA peaks from the entire EDA signal.
- **Minimum EDA (µS)**: the minimum skin conductance (µS) out of all EDA data collected during a measurement session. This value is calculated prior to phasic EDA extraction.
- **Maximum EDA (µS)**: the maximum skin conductance (µS) out of all EDA data collected during a measurement session. This value is calculated prior to phasic EDA extraction.
- **Average EDA (µS)**: the average skin conductance (µS) out of all EDA data collected during a measurement session. This value is calculated prior to phasic EDA extraction.
- **Number of Detected Peaks**: the number the peaks that the EDA signal processing app detects and records for a measurement session.

A.2 App Reported Parameters

The app reports data for each peak as well as for the entire measurement session:

- **Significant Peak Frequency (pks/sec)**: the peak frequency value, calculated by dividing the number of detected peaks by the data duration in seconds.
- **Average Phasic EDA (μS)**: the average value of the amplitudes of all resultant peaks detected during the phasic EDA extraction process.
- **Average Rise Time (sec)**: the average value of the time gaps between the onset times and the next-nearest-times of the respective local maxima.

B. Phasic EDA Peak Extraction

B.1 Phasic EDA Extraction Filter

Once raw EDA data are imported into the signal processing app, the skin conductance level (SCL) and phasic components of the signal are separated. The SCL, which is manifested by a slowly changing signal that visually represents the signal 'baseline,' is calculated by smoothing the EDA signal with a moving average window of a certain width. This process can be expressed as in Equation 1 [46].

$$\mathrm{SCL}(S_n) = \frac{1}{2K} \cdot \sum_{n=k+1}^{S_T-k} \sum_{i=-K}^{K} EDA\ (S_n + i), \tag{1}$$

where S_n is the n^{th} sample, S_T is the total number of samples collected, K is the number of data points before and after S_n for extracting SCL and phasic EDA. $2K+1$ is the full width of the moving average filter window, also referring to the 'window size of the phasic extraction'. The filter window concept is depicted in Figure 16.

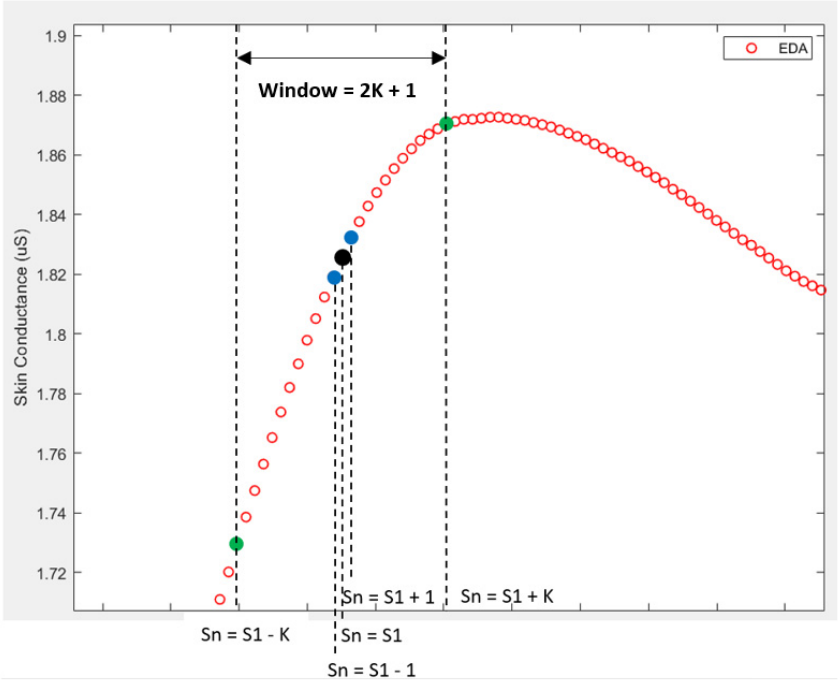

Figure 16. Average filter window depiction for phasic EDA extraction.

After setting the phasic EDA extraction grouping size ($2K + 1$), the phasic EDA component can be determined by subtracting the SCL data from the raw EDA data:

$$Phasic_{EDA}\ (S_n) = EDA\ (S_n) - \mathrm{SCL}(S_n) \quad (2)$$

Figure 17 illustrates the phasic EDA & SCL extraction in one plot. The red line represents the raw EDA data, the black line represents the SCL data, and the blue line represents the phasic EDA component. This extracted phasic EDA signal is the input for the peak detection process implemented in the downstream signal processing app.

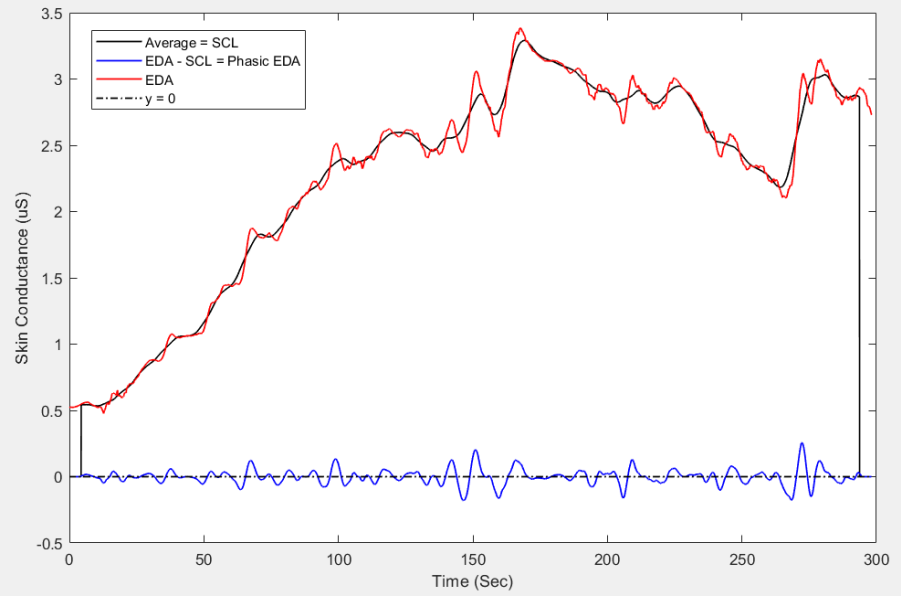

Figure 17. SCL and phasic EDA extraction.

B.2 Effect of Phasic EDA Extraction Filter Window Size

Changes in the phasic EDA extraction (a.k.a., averaging) filter window size significantly influence the resulting phasic EDA signal - see Figure 18. When the window size is too small, the computed SCL follows the phasic activity too closely and cannot exhibit its 'tonic' activity, which is considered to be slowly varying, trending behavior. On the other hand, when the window size is too large, the SCL is less useful for extracting relatively small phasic EDA peaks. Therefore, choosing the right width for the phasic EDA extraction filter is necessary. Usually, SCL is computed over surrounding samples of approximately +/− 4 seconds time period (~ 8 seconds in total) which are centered around one data point [47]. The time interval between each data point is approximately 0.067 seconds. Thus, a phasic EDA extraction filter of width 141 (70 data points before and after one data point) spanning approximately 9.4 seconds was chosen.

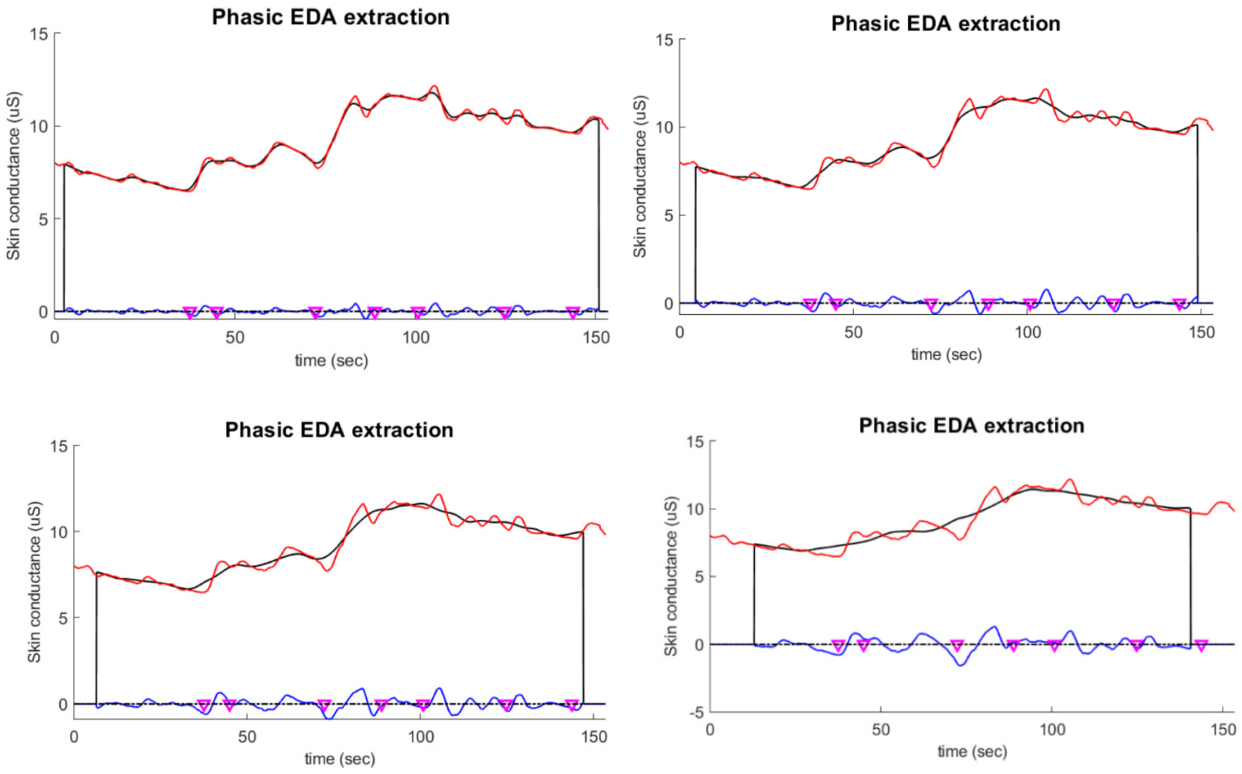

Figure 18. The effect of phasic EDA extraction filter window width (81, 141, 201, and 401 values, moving from the upper left axes to the lower right axes).

C. EDA Peak Detection

Ideally, when $\Delta Phasic_{EDA}\,(S_n)\,/\Delta S_n$ is equal to zero, a local phasic maximum or minimum will be present, assuming a noiseless data set. However, since these data are not continuous, but rather discrete, a sample value may not occur at the exact time of a peak, so choosing a slope threshold value that is just close to zero can narrow down the set of times at which the local maxima can be found. If $\Delta Phasic_{EDA}\,(S_n)\,/\Delta S_n$ is smaller than the parameter slope threshold value, then the signal processing app determines whether the curvature, $(\frac{\Delta}{\Delta S_n})^2 Phasic_{EDA}\,(S_n)$, is negative. If so, the graph is concave down and has a local maximum at the time, *x*, that corresponds to the index, *n*.

C.1 Step 1 – Initial S_n Set for Peak Detection

The initial set of S_n values can be determined by using this slope threshold approach. Figure 19 illustrates an example set of $S_{n_{(1)}}$ values selected by using the slope threshold parameter:

$$S_{n_{(1)}} = \left\{ S_n \in S_{n_{Phasic}} \middle|\ \Delta Phasic_{EDA}\,(S_n)\,/\Delta S_n < SL_t\ ,\ (\frac{\Delta}{\Delta S_n})^2 Phasic_{EDA}\,(S_n) < 0 \right\},$$

where $S_{n_{Phasic}}$represents the S_n values from the phasic EDA data, and SL_t is the slope threshold.

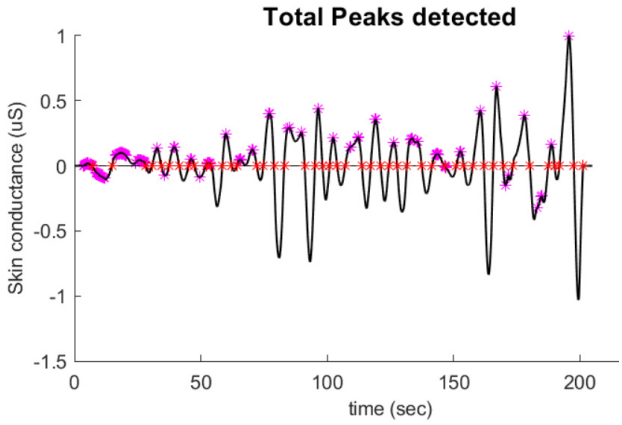

Figure 19. Total peaks, $S_{n_{(1)}}$, detected.

C.2 Step 2 – Second S_n Set for Peak Detection

After the first detection process, one or more S_n values are identified as belonging to $S_{n_{(1)}}$. To omit S_n points that were falsely detected by the slope threshold parameter, one can set the minimum $|Phasic_{EDA}\,(S_n) - Phasic_{EDA}\,(S_{n-1})|$ value and confine the S_n points to the values that meet the condition, $Phasic_{EDA}\,(S_n) > 0$, thereby narrowing down the number of S_n values that can correspond to a given local maximum. Based on this threshold, the following $S_{n_{(2)}}$ set can be selected.

$$S_{n_{(2)}} = \left\{ S_n \in S_{n_{(1)}} \mid |Phasic_{EDA}\,(S_n) - Phasic_{EDA}\,(S_{n-1})| > D_t, Phasic_{EDA}\,(S_n) > 0 \right\},$$

where D_t is the peak distance threshold. Figure 20 illustrates an example set of $S_{n_{(2)}}$ values selected by using the peak distance threshold parameter. Note, in comparison to Figure 19, how multiple spurious S_n values that cluster around some maxima have been reduced to one S_n value per maximum.

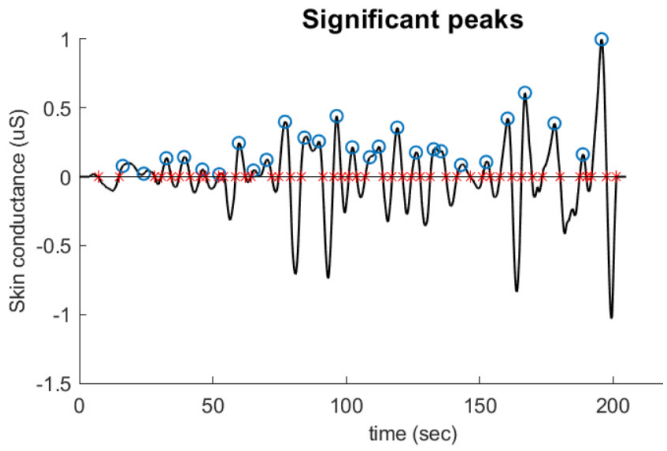

Figure 20. Significant peaks, $S_{n_{(2)}}$, detected.

C.3 Step 3 – Third and Fourth S_n Set for Peak Detection

After selecting $S_{n_{(2)}}$, the EDA signal processing app can determine a single S_n that represents a local maximum by way of a pair of onset/offset values:

$$S_{n_{(3)}} = \left\{ S_n \in S_{n_{(2)}} \mid t_{onset_{(n)}} < t_{S_n} < t_{offset_{(n)}} \right\}$$

and

$$S_{n_{(4)}} = \left\{ S_n \in S_{n_{(3)}} \mid Phasic_{EDA}(S_n) = \max(Phasic_{EDA}(S_{n_{(3)}})) \right\},$$

where $t_{onset_{(n)}}$ and $t_{offset_{(n)}}$ are the onset and offset times for $Phasic_{EDA}(S_n)$, and $\max(Phasic_{EDA}(S_{n_{(3)}}))$ is the maximum value of $Phasic_{EDA}(S_{n_{(3)}})$. Figure 21 illustrates an example set of $S_{n_{(4)}}$ values selected by finding times for maxima via the onset and offset parameters. Notice that only the local maxima, $S_{n_{(4)}}$, were chosen to be analyzed in this research. However, in future work, the data set, $S_{n_{(2)}}$, might be considered to be the set of EDA responses to emotional stimuli due to the psychological information that each non-maximum peak might hold.

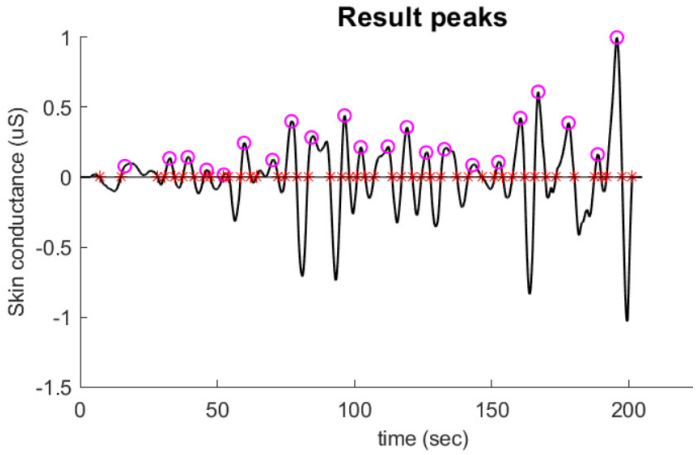

Figure 21. Resultant peaks, $S_{n_{(4)}}$.

D. Parameter Calculation

Figure 22 displays an example phasic EDA peak with its amplitude, $Phasic_{EDA}\ (S_n)$, and rise time. The rise time was calculated by subtracting the onset time, $t_{onset_{(n)}}$, from the peak time, t_{S_n}.

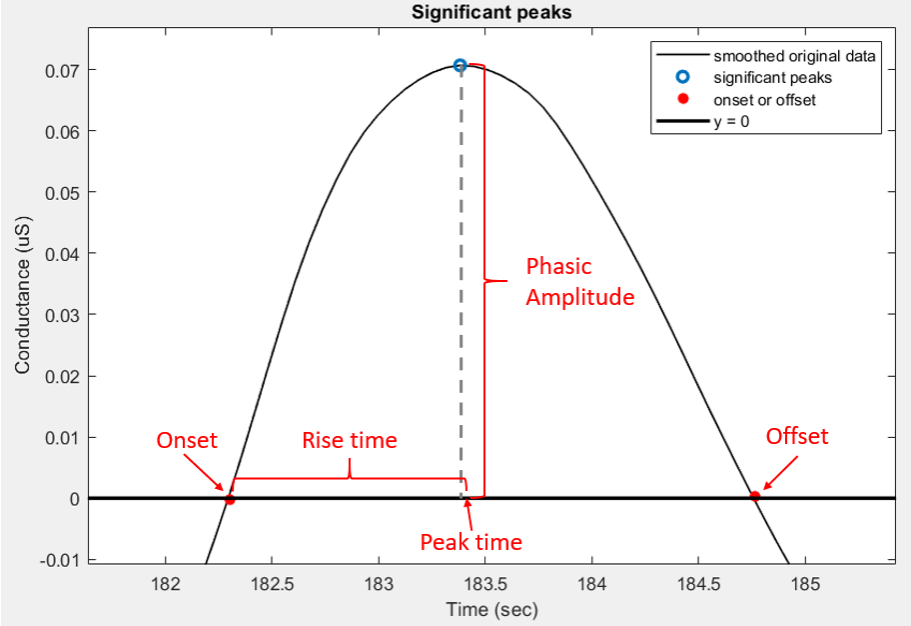

Figure 22. A phasic EDA peak with its amplitude and rise time labeled.

Chapter 6 - Experimental Surveys and Videos

In academic learning and evaluation (test) scenarios, students experience a number of emotional responses to tasks, especially test-related tasks. These emotions can significantly impact student achievement in terms of both learning and grades. Therefore, it is important to identify and, if possible, quantify the emotions involved in learning or test-taking activities.

Academic emotions can be categorized as class-related, learning-related, or test-related emotions [17]. Well-known academic emotions are enjoyment, hope, pride, boredom, anger, anxiety, hopelessness, shame, and sadness [18] [19]. In the work presented here, such academic emotions are identified and quantified using pre-experiment survey questions. These questions address the emotions most often associated with test-taking scenarios, and they also provide 'ground truth' data which can be used to validate 'significant' emotional responses identified by the pen-type EDA system developed for this research. This chapter addresses the pre-experiment survey, videos, and in-experiment surveys that, in aggregate, define the data-gathering session experienced by each human subject involved in this research.

A. Pre-Experiment Survey About Academic Emotions

Prior to the EDA measurements, each subject was asked to identify the emotions they personally associate with academic test scenarios, and they were asked to evaluate these emotions on a scale of 1 to 10, where 1 is a minimal sense of emotion and 10 is an extreme sense of emotion. The purpose of this pre-experiment survey is to determine statistically which emotions can be associated with test-taking for a given student and to validate the significance of emotional responses detected during the measurement sessions. While academic emotions can be class-related, learning-related, or test-related [18] [19] [17], each subject was asked to focus on test-related emotions. The survey itself is included in Appendix B.

In the pre-experiment survey, the emotions can be categorized as positive and negative emotions. The positive emotions are happiness, relaxation, and pride, whereas the negative emotions are sadness, anxiety, hopelessness, anger, shame, and boredom. The emotion 'enjoyment' is often included in EDA research, but 'happiness' is used here instead because it provides a clear positive counterpart for the negative emotion 'sadness.' Note that it is important to include the emotion 'sadness,' because 'sadness' relates to situations where some students psychologically break down during academic tests [18].

B. Emotion-Evoking Videos

The video series employed in each experimental session is approximately 30 minutes long and includes a comforting Mozart music playlist, an extreme parkour video, a jump-scaring ghost video, a video of a pet owner saying goodbye to a sick dog, and a video of near misses while driving on the road. Specific video information is listed in Table 1.

Research Description	Original Title	URL	Video Uploader on YouTube	Latest Access Date
Mozart music playlist	Mozart for Babies Brain Development	https://youtu.be/WjwXxlAyKSI	Kyle Sullivan99	03/27/2020
Extreme parkour	People Are Insane (Intense Edition)	https://youtu.be/9enptNl3KYA	Scoreback	03/27/2020
Jump-scaring	JUMPSCARE CHALLENGE!!!	https://youtu.be/aCDK8dHMoBA	BROS TOP 11	03/27/2020
Saying goodbye	Saying Goodbye to Diesel	https://youtu.be/wVa_PukAmFs	Kyle Schwab	03/27/2020
Near-misses	Craziest Near Misses Compilation 2018	https://youtu.be/85XckznLalo	Dashcam World	03/27/2020

Table 1. Sources of emotion-evoking videos.

During the Mozart music playlist, there is no strong visual stimulation – relaxing Mozart music plays while a static 'sleeping baby' picture is displayed. Only the first 4 minutes of the original Mozart music playlist were used for this research. In the extreme parkour video, where only 2 minutes of the original video were used, scenes of people doing parkour on rooftops are

played; these scenes include tricks such as jumping from roof to roof or hanging on the edge of rooftops. In the jump-scaring video, 6 ghost-like figures pop up unexpectedly, accompanied by loud noises, where an interval of about 15 seconds exists between jump-scaring elements. In the saying-goodbye video, a sick dog named Diesel is being put down by a vet, and the dog's owner says an emotional goodbye. Only the last 2 minutes from the original video were used. Finally, the near-misses videos come from dashcams and helmet cams, where drivers suddenly get surprised by other cars or people that almost cause severe accidents. Only the first 2 minutes from the original video were used.

Note that it is highly unlikely that a student will feel 'jump-scared' during an academic test taking scenario. However, a 'scared' emotion corresponds to a highly elevated sense of anxiety-based stress. Similarly, the extreme parkour video and the 'near misses' video can evoke anxiety-based stress. Sadness is a stress-causing emotion – thus the use of the 'saying goodbye to a pet' video. By using four different videos that address various facets of stress, a researcher can obtain various levels of 'stressed' EDA responses with a goal to differentiate 'stressed' EDA data that are statistically different from 'relaxed' EDA data.

C. Significance of the In-Experiment Survey

'Relaxed' and 'stressed' emotions caused by various events are the targets of the pen-type EDA system employed in this research. However, it is difficult to interpret collected EDA signals and to specifically determine which EDA signals indicate that the respective participants are 'stressed' versus 'relaxed,' partly because everyone's sensitivities to certain emotions and emotion-evoking videos are different. Therefore, ground-truth information based on subjects' own opinions about the relative emotions they felt towards each video is helpful. To that end, an in-experiment survey was conducted to acquire ground-truth information from each participant

regarding the respective videos. More specifically, after watching each video, a subject was asked about the intensity of a given emotion on a scale of 1 to 10. For example, after watching the extreme-parkour video, a subject was asked how ‘anxious’ they felt so that the peaks extracted from their EDA signal could be interpreted in light of that subjective rating, also known as ground truth.

Chapter 7 - Experimental Results and Data Analyses

A. Survey Response Statistics

A.1 Pre-Experiment Survey Results

Table 2 contains aggregated results from the pre-experiment surveys, where each subject rated their level of each emotion associated with test taking. For columns 1 to 10, the number of subjects out of 36 who chose each rating are noted. An emotional score was determined in each case:

$$\text{Emotional Score} = \sum_{index\,=\,1}^{10} index \cdot count \tag{3}$$

	1	2	3	4	5	6	7	8	9	10	Total Count	Emotional Score	Percentage (%)
Happiness	23	2	3	0	1	3	4	0	0	0	36	87	9.0
Relaxation	20	3	0	2	1	3	4	3	0	0	36	109	11.3
Pride	14	0	3	3	7	3	3	2	0	1	36	135	13.9
Sadness	25	0	1	6	2	0	0	1	0	1	36	80	8.3
Anxiety	3	0	1	4	3	2	6	12	3	2	36	234	24.2
Hopelessness	20	1	2	2	3	3	4	0	0	1	36	107	11.1
Anger	25	1	1	2	5	1	0	0	0	1	36	79	8.2
Shame	29	1	1	2	3	0	0	0	0	0	36	57	5.9
Boredom	23	3	2	3	1	2	0	2	0	0	36	80	8.3

Table 2. Counts for academic emotions chosen by 36 subjects and the average index for each emotion.

The relative percentage of each score was calculated as well. These percentages are illustrated in the pie chart in Figure 23, where anxiety takes up 24 %, followed by pride (14%), relaxation (11%), hopelessness (11%), happiness (9%), boredom (9%), sadness (8%), anger (8%), and shame (6%). These numbers indicate that students are strongly influenced by anxiety while viewing video content, and it is therefore reasonable to assume that such anxiety can be triggered by test content and therefore negatively affect a student's academic performance.

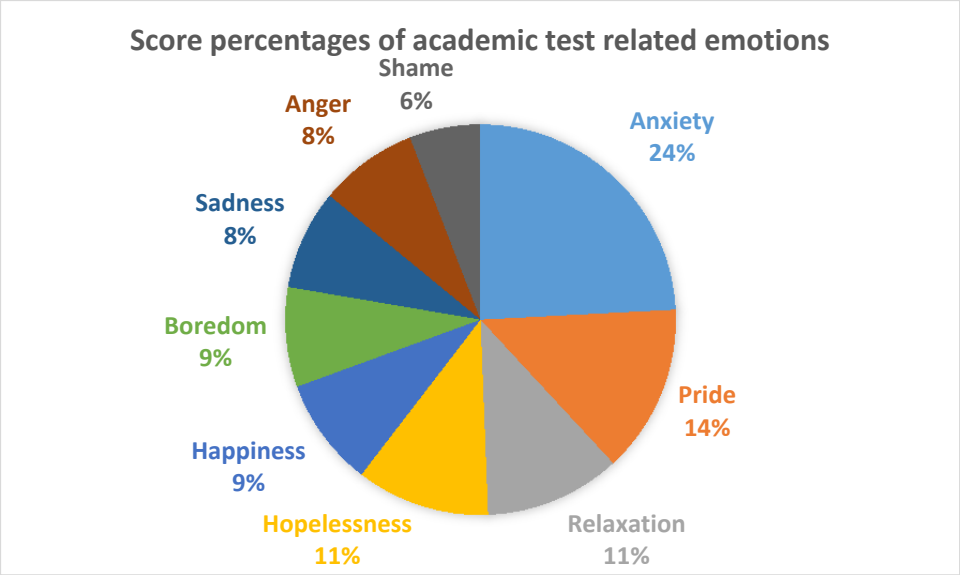

Figure 23. Pie chart illustrating relative percentages of academic test-related emotions identified by participants.

A.2 In-Experiment Survey Results

For the in-experiment survey, each subject's rating regarding their perceived level of stress was tallied following each of the five different videos, where a rating of 1 would mean a minimal sense of emotion and a rating of 10 would mean an extreme sense of emotion. For example, out of the 36 subjects, the number of subjects who offered a relaxation rating of '7' after the Mozart music video was 11 – see Table 3. From the table, it is apparent that some emotion-evoking videos were effective in stimulating the designated emotions, whereas some were not. For example, the emotion-evoking ability of the 'near-misses' video was rated relatively low compared to the parkour video. As indicated in this in-experiment survey, the range of phasic EDA amplitudes for the 'near-misses' video should overlap significantly with the corresponding range for the 'relaxed' emotion evoked by the Mozart music (e.g., see Figure 24

and its accompanying text), which in essence disqualifies the phasic EDA amplitudes for the 'near-misses' video to be categorized into the 'stressed' group.

	1	*2*	*3*	*4*	*5*	*6*	*7*	*8*	*9*	*10*	*Total*
Mozart music	0	0	1	1	3	3	11	10	3	4	36
Parkour	2	1	4	3	1	2	9	11	1	2	36
Jump-scaring	2	3	2	5	4	5	3	6	5	1	36
Saying goodbye	0	1	2	2	4	5	7	6	6	3	36
Near-misses	3	2	5	5	3	8	5	3	2	0	36

Table 3. In-experiment survey results for each video.

As mentioned previously, in-experiment survey information plays an important role when dividing the entire collection of EDA signal data into two groups ('stressed' versus 'relaxed'), where the 'stressed' group only consists of data from subjects who offered a "5" or above after the parkour, jump-scaring, saying goodbye, or near-misses video; and the 'relaxed' group consists of data from subjects who offered a "5" or above after the Mozart music playlist. It is helpful to divide these response data into two groups to obtain 'ground-truth' knowledge of the 'stressed' group, which can be used to establish a training model for stress detection – see Chapter 8.

B. EDA Parameter Statistics

B.1 Standardization

An individual's physical characteristics, such as skin thickness, affect the amplitude ranges for their acquired EDA data. Standardization of these datasets is therefore necessary to enable comparisons of data acquired from different individuals. One means to achieve such standardization is to divide each EDA data parameter (e.g., amplitude) by the corresponding individual's maximum EDA signal value. For this work, the average of an individual's three highest EDA signal values was used for that purpose, which helps to compensate for outliers.

B.2 Phasic EDA Amplitude Data

Figure 24 displays box plots of 'standardized' phasic amplitude data for the five emotion-evoking videos. For convenience, each video is numbered from 1 to 5, where the 'Mozart music playlist' is 1st, the 'parkour' video is 2nd, the 'jump-scaring' video is 3rd, the 'saying goodbye' video is 4th, and the 'near-misses' video is 5th. To create a box plot, all of the phasic amplitudes that relate to each video are aggregated for all of the study participants. Then, six pieces of information are calculated for that collection of amplitudes: the minimum, maximum, average, median, first quartile, and third quartile. In this context, a "quartile" means a value that serves as a threshold for one quarter of the numerical set. For example, the first quartile means the value above the minimum that serves as the upper threshold for the lowest quarter of the numerical values, whereas the third quartile means the value below the maximum that serves as the lower threshold for the highest quarter of the numerical values. The bounds for the first and third quartiles are illustrated using 'whiskers' that extend way from the 'box,' where the lower whisker extends from the minimum to the bottom of the box, and the higher whisker extends from the top of the box to the maximum. The box itself illustrates the bounds for the remaining 50% of the numerical values, where the line inside the box represents the median (the second quartile for the numerical values) and the 'x' indicates the average value. Small circles above/below the bounding whiskers represent outliers.

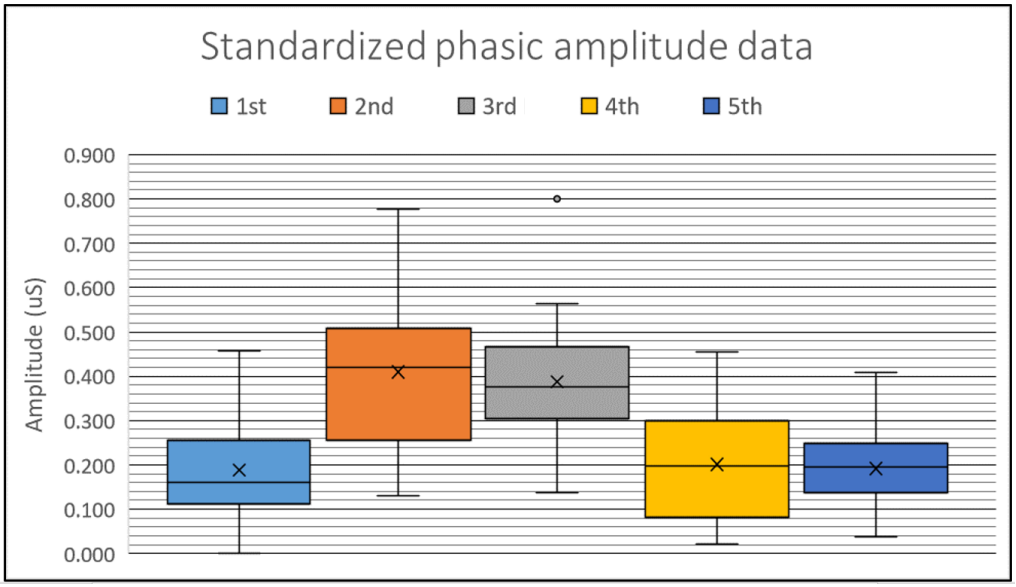

Figure 24. Box plots of standardized phasic amplitude data for each video.

Table 4 contains detailed information about those box plots. As noted in the table, the amplitude range (quartile 1 - quartile 3) for the 1st video (0.1234 – 0.2357 µS) does not overlap with the range for the 2nd video (0.2612 – 0.5046 µS) or the 3rd video (0.3098 – 0.4625 µS). This indicates the EDA data of the 1st video are statistically different than the EDA data for both the 2nd and 3rd videos. However, the amplitude range for the 1st video significantly overlaps with the ranges for the 4th and 5th videos. Therefore, it is statistically difficult to differentiate the 'control' EDA data set, which represents a 'relaxed' emotion, from the 4th and the 5th data sets. Therefore, the EDA data affiliated with the 2nd and 3rd videos are merged into one grouping, i.e., the 'stressed' data set, as opposed to the 'relaxed' data set associated only with the 1st video.

	Average	*stdev*	*Min*	*Max*	*Quartile 1*	*Quartile 3*	*Median*	*Skewness*
1st Video	0.1881	0.1189	0.0002	0.4569	0.1234	0.2357	0.1594	0.9355
2nd Video	0.4097	0.1766	0.1305	0.7763	0.2612	0.5046	0.4192	0.2233
3rd Video	0.3878	0.1263	0.1385	0.8002	0.3098	0.4625	0.3757	0.6965
4th Video	0.2015	0.1242	0.0213	0.4545	0.0828	0.2961	0.1987	0.3738
5th Video	0.1917	0.0912	0.0370	0.4089	0.1377	0.2412	0.1953	0.1312

Table 4. Table of phasic amplitude data for a 141-wide filter window.

A two-tailed mean *t* test with a significance level of 0.01 was conducted for the relaxed versus stressed groups to see if their averages were statistically distinct. As indicated in Table 5, the null hypothesis (H_0) for this mean *t* test was the following:

H_0 = 'The mean EDA amplitude for the relaxed group and the mean EDA amplitude for the stressed group are the same'

The result of the two-tailed mean *t* test was to reject the null hypothesis, indicating there is evidence that the mean amplitudes of the 'relaxed' data set and the 'stressed' data set are statistically different. It therefore makes sense to differentiate those two groups based on their corresponding amplitude measures, which also implies that further analysis based on these two distinct groups is warranted.

Two-Tailed t Test	***0.01 Significance Level***	
Data Set	*Relaxed*	*Stressed*
Number of Values	839	1325
$\boldsymbol{H_0}$	$M_{relaxed} = M_{stressed}$	
t value	-16.46	
p value	<0.0001	
t test result	Reject the null hypothesis	
Interpretation	EDA amplitudes for 'relaxed' data and 'stressed' data are statistically different	

Table 5. Two-tailed mean *t* test for the 'relaxed' versus 'stressed' data sets.

B.3 Slope Data

Next, box plots and a corresponding table were created based on the 'slope' data – see Figure 25 and

Table 6. Here, slope means 'peak amplitude / rise time (μS/sec)'. The slope data range (min, max) numbers imply that the responses to the 1st video are statistically different from the

responses to the 2nd and 3rd videos, since the slope data ranges do not overlap with each other. However, unlike the phasic amplitude data, more outliers exist, making this parameter less desirable to use for classifying data sets into 'relaxed' or 'stressed' categories.

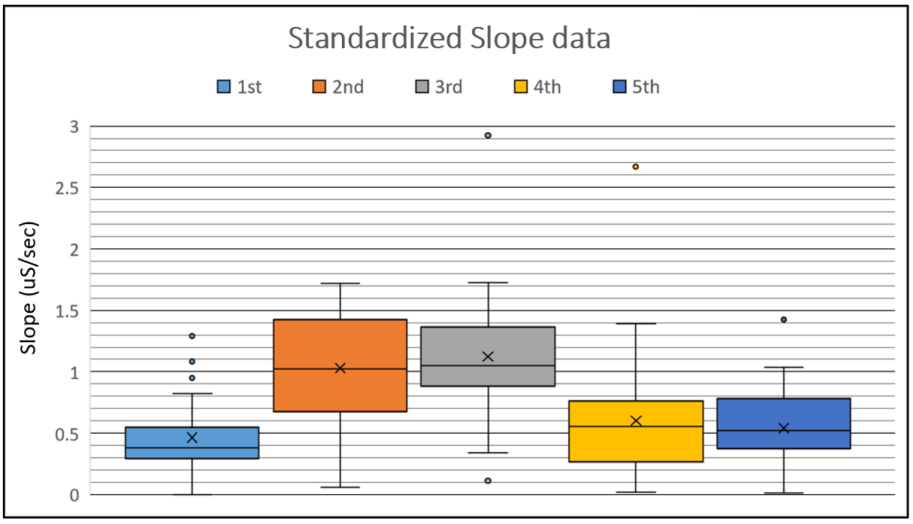

Figure 25. Box plots of standardized slope data for a 141-wide filter window.

	Average	*stdev*	*Min*	*Max*	*Quartile 1*	*Quartile 3*	*Median*	*Skewness*
1st Video	0.4643	0.2983	0.0003	1.2923	0.2969	0.5399	0.2983	0.2983
2nd Video	1.0282	0.4364	0.0587	1.7207	0.6929	1.4182	0.4364	0.4364
3rd Video	1.1236	0.4759	0.1140	2.9243	0.9015	1.3260	0.4759	0.4759
4th Video	0.6022	0.4812	0.0170	2.6687	0.2718	0.7583	0.4812	0.4812
5th Video	0.5418	0.3129	0.0094	1.4256	0.3886	0.7396	0.3129	0.3129

Table 6. Table of standardized slope-time data for a 141-wide filter window.

B.4 Rise Time Data

Next, box plots and a table were created based on 'rise time' data – see Figure 26 and Table 7. As indicated by the box plots, the rise-time data ranges for each video overlap significantly, and a number of outliers exist, making the 'rise time' parameter unsuitable as a 'stress' indicator.

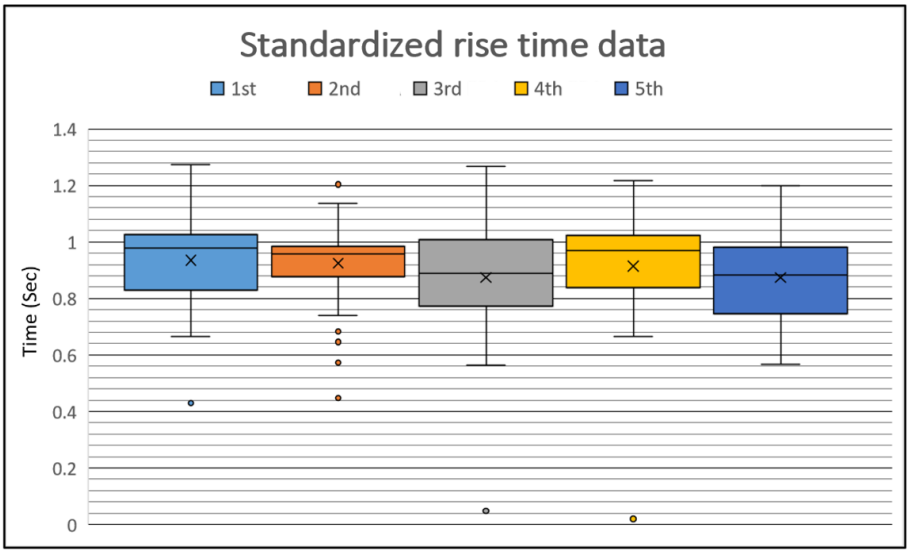

Figure 26. Box plots of standardized rise time data for a 141-wide filter window.

	Average	*stdev*	*Min*	*Max*	*Quartile 1*	*Quartile 3*	*Median*	*Skewness*
1st Video	0.935448	0.158162	0.429422	1.272182	0.860538	1.020527	0.982235	-0.90918
2nd Video	0.923933	0.155182	0.448494	1.213177	0.877893	0.98377	0.961148	-1.08898
3rd Video	0.873878	0.209028	0.047678	1.267681	0.775974	1.006299	0.878935	-1.60458
4th Video	0.914757	0.199017	0.02011	1.216842	0.84327	1.020638	0.953	-2.70312
5th Video	0.874327	0.150398	0.568213	1.200386	0.75739	0.981311	0.883691	-0.07596

Table 7. Table of standardized rise time data for a 141-wide filter window.

B.5 Peak Frequency Data

Finally, Figure 27 and Table 8 display results for the standardized 'peak frequency' data. The 'peak frequency' parameter describes the number of peaks (occurrences) per time that are detected by the EDA signal processing app within the data-collection time frame. In other words, the peak frequency values were calculated by dividing the number of detected peaks by the data duration in seconds. This parameter was also not a good candidate for a 'stress' indicator, for reasons similar to those stated above for the 'rise time' parameter.

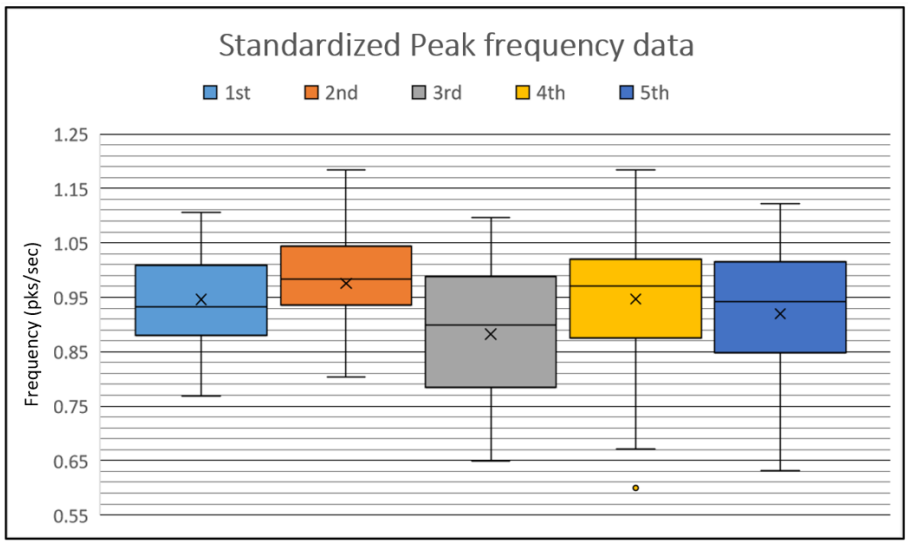

Figure 27. Box plots of standardized peak frequency data for each video.

	Average	*stdev*	*Min*	*Max*	*Quartile 1*	*Quartile 3*	*Median*	*Skewness*
1st Video	0.9455	0.0883	0.7681	1.1053	0.8849	1.0057	0.9322	0.2274
2nd Video	0.9754	0.0879	0.8026	1.1833	0.9356	1.0417	0.9829	-0.2061
3rd Video	0.8821	0.1256	0.6492	1.0958	0.7926	0.9858	0.8982	-0.1842
4th Video	0.9471	0.1126	0.6000	1.1833	0.8776	1.0132	0.9703	-0.8471
5th Video	0.9198	0.1230	0.6309	1.1220	0.8481	1.0128	0.9423	-0.6071

Table 8. Table of standardized peak frequency data for the 141-wide filter window.

Chapter 8 - Stress Detection

In this chapter, classification of test data into 'relaxed' versus 'stressed' states is addressed following algorithm training based on ground-truth data. Two different 'stress detection' phases are presented. In the first phase, data sets were chosen with training-to-test ratios of 80/20 (i.e., 80% of the amplitudes used for training, and 20% of the amplitudes used for testing) and 50/50 to compare their 'cross-validation' performance. In the second phase, the 'stress detection' performance was tested by using each subject's whole data set instead of creating 'artificial' test data sets in which each data point is randomly chosen for different individuals. The flow charts for the different 'stress detection' tests are offered in Figure 28, Figure 29, and Figure 33.

A. Stress Detection and Cross-Validation

A.1 Stress Detection Models

As mentioned in the previous chapter, the total EDA data set was divided into two statistically different groups. The first group, considered 'ground-truth' relaxed data, was comprised of EDA data acquired from the 34 subjects who rated their relaxation level at 5 or above after listening to the 'Mozart playlist' (see Table 3). The second group, considered 'ground-truth' stressed data, was comprised of EDA data acquired from the 26 subjects who rated their stress level at 5 or above after watching the 'parkour' and/or 'jump-scaring' videos. The rest of the EDA data were not used in either training or testing the detection model because those data were collected from subjects who rated their stress levels at less than 5, thus failing to provide 'ground-truth' stress data.

Two generalized extreme value (GEV) models were selected for the 'relaxed' and 'stressed' states after visual inspection of the amplitude histograms that were created using the

'relaxed' and 'stressed' training data sets. These GEV models were assessed with a chi-squared goodness-of-fit test and were then cross-validated by the 'test' data sets in downstream steps.

A.2 Training/Test Data (80/20 Ratio) and Detection Flow Diagram

Given the availability of 780 'relaxed' and 780 'stressed' ground-truth data (EDA phasic amplitudes), some (630 values) were chosen for the training data set and some (150 values divided into 5 sets of 30) were chosen for the test data set – see Figure 28. This provides about an 80/20 ratio of training data to test data. Thus, in each test 'relaxed' data set, for example, there were 30 randomly chosen data points. This means that each test data set did not completely arise from a single subject's data, but rather 30 randomly chosen data points from 20% of the entire ground-truth 'relaxed' data set were merged into one test data set. The same proportions of training and test data sets were created for the 'stressed' group using the same method. These randomly picked training data sets and test data sets were created 14 more times so that there were 15 different training-test data configurations. Thus, in total, there were 15 different training models and 75 different test data sets. For each of the 15 different training models, 5 test sets of 30 values were designated.

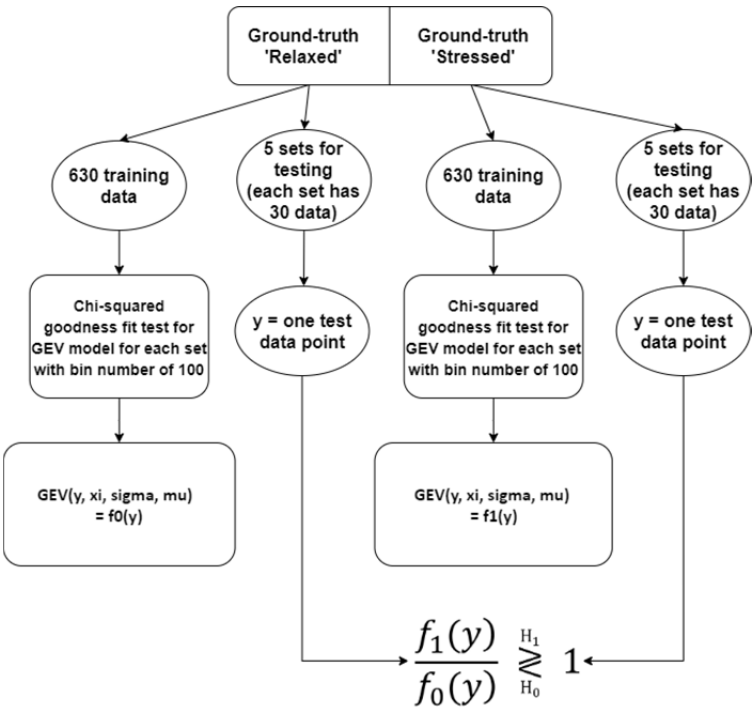

Figure 28. Stress detection flow chart for a training-to-testing data ratio of 80/20.

A.3 Training/Test Data (50/50 Ratio) and Detection Flow Diagram

Training/test data with a 50/50 ratio were also chosen (see Figure 29) in a manner similar to the 80/20 training/test sets described in the previous section so that the relative performances of the approaches could be compared. However, for the 50/50 ratio as applied to both the 'relaxed' and 'stressed' data, 394 data points were randomly chosen to be the 'training' data, and 390 data points were randomly chosen to be the 'test' data. Those 390 data were divided into 13 different test sets so that each test set had 30 data points. For the 50/50 ratio, 15 different training models were created, and for each of the 15 different training models, 13 different test data sets were designated.

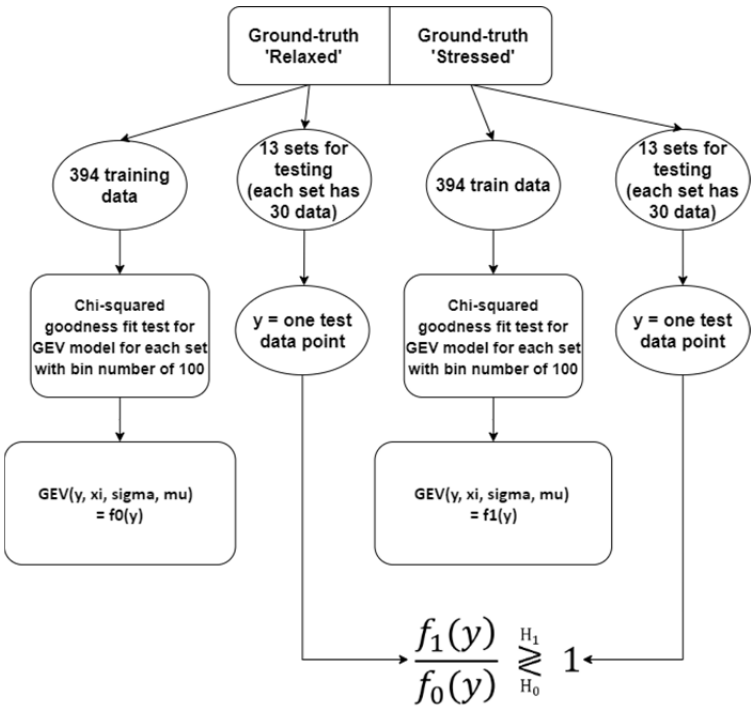

Figure 29. Stress detection flow chart for a training-to-testing data ratio of 50/50.

A.4 Generalized Extreme Value (GEV) Model and Chi-Squared Goodness-of-Fit Test

Normalized histograms (i.e., where each histogram has a total area of one) with 100 bins each were created using EDA amplitudes from the 'relaxed' and 'stressed' training data sets. This normalization allowed theoretical probability density functions (PDFs) to bit fitted to those distributions and act as statistical models. As displayed in Figure 30, generalized extreme value (GEV) models 'visually' fit the normalized histograms of both the 630 'relaxed' and the 630 'stressed' training data (amplitudes). The GEV probability distribution function is described as

$$\text{GEV}(y, \xi, \sigma, \mu) = \frac{1}{\sigma}\, t(y)^{\,\xi+1} e^{-t(y)}, \tag{4}$$

$$\text{where } t(y) = \begin{cases} (1 + \xi(\frac{y-\mu}{\sigma}))^{-1/\xi} \; if \; \xi \neq 0 \\ e^{-(y-\mu)/\sigma} \; if \; \xi = 0 \end{cases}$$

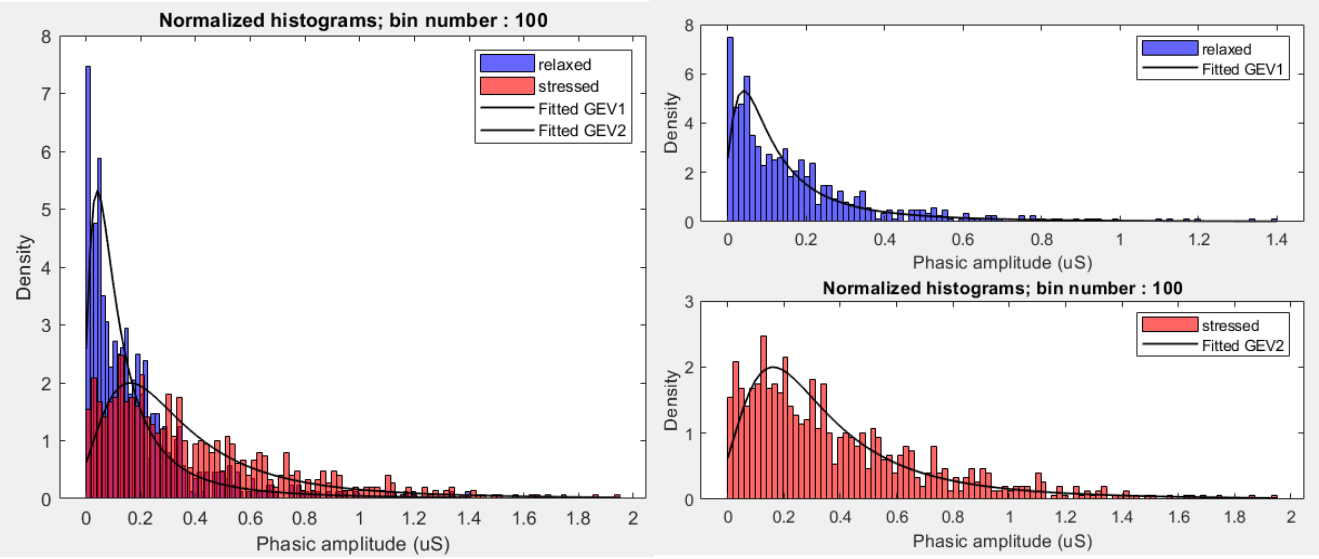

Figure 30. An example of a GEV model fitted to the normalized training data.

Here, y is one data point, ξ is a shape parameter, σ is a scale parameter, and μ is a location parameter. Chi-squared goodness-of-fit tests were used to optimize the fits between 15 different GEV models and their corresponding 15 training sets. In each chi-squared goodness-of-fit test [48], the statistics, which is referred to as 'Z', from both sets of data were calculated using

$$Z = \sum_{j=1}^{m} \frac{|H_j - np_j|^2}{np_j} \tag{5}$$

where H_j is the number of data that fall into the j^{th} bin, n is the total number of these data,and p_j is the probability that the data point y_j falls into the j^{th} bin. The probability p_j is denoted by

$$p_j = P\left(e_j \le y_j \le e_{j+1}\right) = \int_{e_j}^{e_{j+1}} f(y)dy \quad (6)$$

where e_j and e_{j+1} are the bin edges. This probability is determined by applying a cumulative distribution function (CDF) over the interval of e_j to e_{j+1}, where the CDF is defined as

$$F(x) = \int_{-\infty}^{x} f(y)\, dy$$

where $f(y)$ is a probability density function. Thus, the CDF of the selected GEV model is

$$F(x) = \int_{-\infty}^{x} GEV(y, \xi, \sigma, \mu)\, dy \quad (7)$$

The probability $p_j = \mathrm{P}\left(a \le y_j \le b\right)$, can be determined by $\int_a^b GEV(y, \xi, \sigma, \mu)\, dy$. Here, '$a$' and '$b$' correspond to e_j and e_{j+1}, respectively.

Based on Equation (5) ~ (7), the *Zx* values (*Z* values for the 'relaxed' data) and *Zy* values (*Z* values for the 'stressed' data) were calculated and compared with the threshold, *Z*α. If a Z value is smaller than *Z*α, it indicates that the suggested GEV model is a good fit to the data. The *Z*α is chosen so that the following equation is satisfied:

$$P(Z > Z\alpha) = \alpha \quad (8)$$

where α is the probability of rejecting the suggested model. In this study, α was chosen to be 0.05. Table 9 contains *Zx* and *Zy* values for each of the 15 different training models for the 80/20 scenario. All models pass the chi-squared goodness-of-fit test since their *Z* values are smaller than *Z*α = 123.22, indicating these GEV models are good fits. The same chi-squared goodness-of-fit tests were conducted for the models used in the 50/50 ratio tests. The *Z* values for these 50/50 ratio tests can be found in Appendix E.

	Test 1	Test 2	Test 3	Test 4	Test 5	Test 6	Test 7
ξ_relaxed	5.73E-01	5.59E-01	5.85E-01	5.92E-01	5.49E-01	6.08E-01	5.59E-01
σ_relaxed	7.93E-02	7.87E-02	7.82E-02	7.63E-02	8.07E-02	7.91E-02	7.78E-02
μ_relaxed	7.20E-02	7.29E-02	7.11E-02	6.96E-02	7.47E-02	7.12E-02	7.19E-02
ξ_stressed	3.30E-01	3.45E-01	3.31E-01	3.56E-01	3.29E-01	3.19E-01	3.35E-01
σ_stressed	1.93E-01	2.01E-01	1.98E-01	1.95E-01	1.96E-01	2.01E-01	1.95E-01
μ_stressed	2.13E-01	2.19E-01	2.16E-01	2.11E-01	2.15E-01	2.21E-01	2.17E-01
Zx	4.02E+00	3.90E+00	3.96E+00	3.71E+00	4.22E+00	3.55E+00	4.01E+00
Zy	2.25E+00	2.29E+00	2.61E+00	2.42E+00	2.74E+00	2.67E+00	2.69E+00

	Test 8	Test 9	Test 10	Test 11	Test 12	Test 13	Test 14	Test 15
ξ_relaxed	5.85E-01	5.71E-01	5.97E-01	5.42E-01	6.00E-01	5.82E-01	5.41E-01	5.90E-01
σ_relaxed	7.94E-02	8.20E-02	7.99E-02	8.09E-02	7.99E-02	7.80E-02	8.22E-02	7.92E-02
μ_relaxed	7.19E-02	7.40E-02	7.19E-02	7.44E-02	7.13E-02	7.07E-02	7.56E-02	7.11E-02
ξ_stressed	3.19E-01	3.26E-01	3.50E-01	3.46E-01	3.45E-01	3.38E-01	3.49E-01	3.27E-01
σ_stressed	1.99E-01	1.99E-01	1.96E-01	1.98E-01	2.02E-01	1.99E-01	2.03E-01	2.01E-01
μ_stressed	2.19E-01	2.19E-01	2.15E-01	2.18E-01	2.19E-01	2.19E-01	2.19E-01	2.19E-01
Zx	3.82E+00	3.77E+00	3.62E+00	4.34E+00	3.57E+00	4.02E+00	4.19E+00	3.78E+00
Zy	2.77E+00	2.23E+00	2.08E+00	2.39E+00	2.26E+00	2.47E+00	2.19E+00	2.53E+00

Table 9. Estimated GEV model parameters and *Z* values for 15 different data sets (80/20).

The fitted GEV models corresponding to the estimated values from 'test1' in Table 9 for the 'relaxed' and 'stressed' data are noted as examples in Equation (9). Similarly, 14 other GEV models were established like these examples based on the estimated parameters.

$$\text{Relaxed: } \text{GEV}(y, \xi, \sigma, \mu) = \text{GEV}(y, 0.5725, 0.0793, 0.0720) = f_0(y) \quad (9)$$

$$\text{Stressed: } \text{GEV}(y, \xi, \sigma, \mu) = \text{GEV}(y, 0.3303, 0.1933, 0.2134) = f_1(y)$$

A.5 Likelihood Ratio Test for Cross-Validation

After establishing GEV models for fifteen sets of relaxed and stressed data (refer to Figure 28 and Figure 29), a null hypothesis (H_0) and an alternative hypothesis (H_1) are made:

H_0= the selected data point, y, belongs to the relaxed data set

H_1 = the selected data point, y, belongs to the stressed data set

After establishing these hypotheses, the acceptance of either H_0 or H_1 depends on a likelihood ratio test, where H_1 is accepted when the likelihood ratio, $f_1(y)/ f_0(y)$, is bigger than 1, and H_0 is accepted when the ratio is smaller than 1:

$$\frac{f_1(y)}{f_0(y)} \underset{H_0}{\overset{H_1}{\gtrless}} 1 \tag{10}$$

This likelihood ratio test is based on two assumptions: 1) 'relaxed' and 'stressed' data sets are equally likely, and 2) a uniform cost function exists, where the risk and error rates are equal. The likelihood ratio test in Equation 10 has been widely used to detect or classify data [49-51].

For example, if data point 1 from a test set (1) is $y_{(1)}^{1}$, a likelihood ratio test is conducted for each data point, $y_{(1)}^{1}$, $y_{(1)}^{2}$, …, $y_{(1)}^{30}$, since there are 30 data points in one test set. Then, the test is repeated four more times (to achieve testing for the rest of the 20% in the 80/20 scheme), for both the relaxed and stressed groups. The likelihood ratio for each set is then calculated by multiplying all thirty $y_{(n)}^{1}$, $y_{(n)}^{2}$,…, $y_{(n)}^{30}$ together since they are independent samples. The product of this multiplication becomes $f_0(y)$ if $y_{(n)}$ values are from the 'relaxed' group or $f_1(y)$ if they are from the 'stressed' group. Finally, the whole process is repeated 14 more times. Eventually, there are 15 different training GEV models with which 75 different test data sets are tested.

In Appendix E, Table 11 through Table 15 display each likelihood ratio for the relaxed and stressed test sets. All 'relaxed' test sets have a ratio smaller than 1, indicating H_0 was accepted. This means these test sets are determined to be 'relaxed' by the likelihood ratio test. Also, all stressed test sets have a ratio bigger than 1, indicating H_1 was accepted. This means these test sets are determined to be 'stressed' by the ratio test.

A.6 Confusion Matrix for the 80/20 Ratio

Based on the likelihood ratio test results, a confusion matrix was created (see Figure 31) for the 'relaxed' and 'stressed' data sets in the context of the 80/20 training/testing ratio. In this scenario, a 'positive' result means that an EDA amplitude is determined to be from a 'stressed' person, and a 'negative' result means that an EDA amplitude is determined to be from a 'relaxed' person. Sensitivity was calculated as 100% · TP/(TP+FN); specificity was calculated as 100% · TN/(FP+TN); precision was calculated as 100% · TP/(TP+FP); and accuracy was calculated as 100% · (TP+TN)/(TP+FN+FP+TN).

		Predicted Class		
		Stressed	**Relaxed**	
Actual Class	**Stressed**	TP = 75	FN = 0	Sensitivity 100
	Relaxed	FP = 0	TN = 75	Specificity 100
		Precision 100	Negative Predicted Value 100	Accuracy 100

TP = True Positive, FP = False Positive, FN = False Negative, TN = True Negative

Figure 31. Confusion matrix for 'relaxed' versus 'stressed' classifications with an 80/20 ratio.

The confusion matrix in Figure 31 states a classification performance with a 100% sensitivity, specificity, precision, and accuracy under two conditions: 1) the ratio of training to test data is 80 to 20; and 2) each test data set contains 30 randomly chosen data points from the entire ground-truth data set instead of from individual subjects. This performance can change when the training-to-test ratio changes or the test data sets change.

A.7 Confusion Matrix for the 50/50 Ratio

As mentioned previously, the classification performance of this system can vary based on the training-to-testing ratio. To compare the system performance against the 'stress detection' test with an 80/20 ratio, a similar test was done with a 50/50 ratio, and its confusion matrix is contained in Figure 32. As displayed in the matrix, the sensitivity, specificity, precision, and accuracy changed to 98.46 %, with 3 false negative and 3 false positive cases occurring out of 195 cases.

		Predicted Class		
		Stressed	**Relaxed**	
Actual Class	**Stressed**	TP = 192	FN = 3	Sensitivity 98.46
	Relaxed	FP = 3	TN = 192	Specificity 98.46
		Precision 98.46	Negative Predicted Value 98.46	Accuracy 98.46

TP = True Positive, FP = False Positive, FN = False Negative, TN = True Negative

Figure 32. Confusion matrix for 'relaxed' versus 'stressed' classifications with a 50/50 ratio.

B. Stress Detection for Each Subject

To test 'stress detection' performance for each subject, individuals' data were used as 'test' sets instead of using randomly chosen test data. The 20 individuals who indicated a 5 or above for all the Mozart music playlist, parkour, and jump-scaring videos were chosen for these 'test' data. The EDA data from the Mozart music playlist, parkour, and jump-scaring videos are referred to as 'relaxed', 'stressed 1', and 'stressed 2' data, respectively. Thus, from one subject, three different EDA responses are taken, and therefore there are 60 different test cases in total. As illustrated in Figure 33, 394 'training' data are randomly picked from ground-truth data for both the 'relaxed' and 'stressed' states, as in previous tests. Only one 'training' model for each 'relaxed' and 'stressed' state is selected. The selected training models are GEV(y, 0.584, 0.0837, 0.0741) for the 'relaxed' state and GEV(y, 0.386, 0.204, 0.213) for the 'stressed' state. These two models passed the chi-squared goodness-of-fit test and were used in all 60 tests.

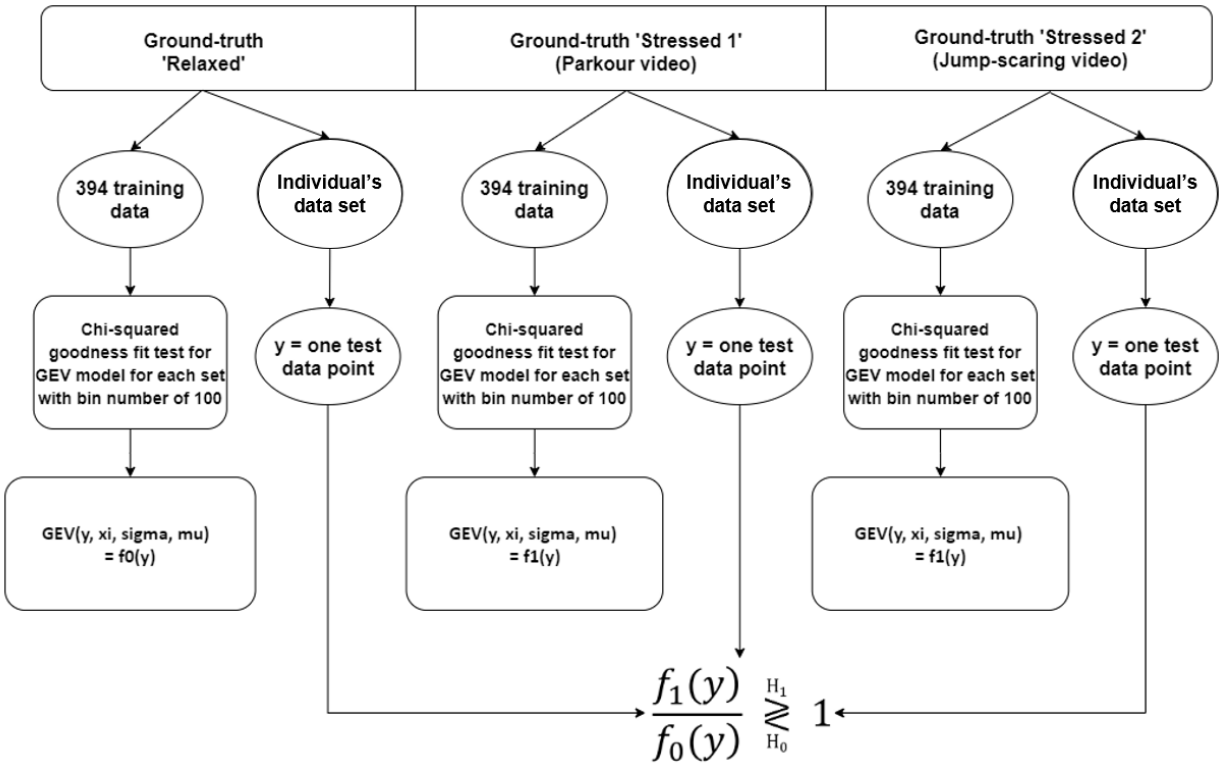

Figure 33. Stress detection flow chart as applied to an individual's data.

The likelihood ratio tests were conducted using the selected training models and these individuals' test data. The 'relaxed' test data set was paired against both the 'stressed 1' and 'stressed 2' test data sets, respectively, to derive the confusion matrices in Figure 34 and Figure 35.

		Predicted Class		
		Stressed 1	**Relaxed**	
Actual Class	**Stressed 1**	TP = 15	FN = 5	Sensitivity 75
	Relaxed	FP = 2	TN = 18	Specificity 90
		Precision 88.24	Negative Predicted Value 78.26	Accuracy 82.5

TP = True Positive, FP = False Positive, FN = False Negative, TN = True Negative

Figure 34. Confusion matrix for a 'relaxed' versus 'stressed 1' classification.

		Predicted Class		
		Stressed 2	**Relaxed**	
Actual Class	**Stressed 2**	TP = 17	FN = 3	Sensitivity 85
	Relaxed	FP = 2	TN = 18	Specificity 90
		Precision 89.47	Negative Predicted Value 85.71	Accuracy 87.5

TP = True Positive, FP = False Positive, FN = False Negative, TN = True Negative

Figure 35. Confusion matrix for a 'relaxed' and 'stressed 2' classification.

As indicated in Figure 34 and Figure 35, the classification performance for the ‘relaxed’ and ‘stressed 1’ data sets was 75% for sensitivity, 90% for specificity, 88.24% for precision, and 82.5% for accuracy. The performance for the ‘relaxed’ and the ‘stressed 2’ data sets was 85% for sensitivity, 90% for specificity, 89.47% for precision, and 87.5% for accuracy. This implies that the classification performance is slightly better when ‘stressed’ test data are chosen from the EDA responses for the ‘jump-scaring’ video instead of the ‘parkour’ video. Moreover, the classification performance in each case is not as good as the performance achieved using the randomly chosen test sets. However, this result indicates that the pen-type EDA sensing system can detect whether a person is stressed or not with an average accuracy of 85% for the videos employed in this study, assuming that their emotional state has been independently self-verified as ‘relaxed’ or ‘stressed.’

Chapter 9 – Conclusion

A. Overview and Results

A pen-type electrodermal activity (EDA) sensing system was implemented as a possible means to detect psychological stress in academic test-taking scenarios. The sensing electrodes are attached to a pen-mounted 'trainer,' which provides a fixed handgrip so that every subject who holds the unit interfaces with the thumb- and finger-located sensors in a controlled manner. These electrodes are connected to a printed circuit board (PCB) that contains a voltage divider and a lowpass filter for each signal. An Arduino Nano unit interfaces to the PCB, and a USB isolator eliminates any ohmic electrical connections for the power source and the data lines so as to protect both the user and the downstream electronics.

In this research, minor psychological stress was evoked using four different videos: a parkour video, a jump-scaring video, a saying-goodbye video, and a near-misses video. The control emotion ('relaxed') was induced with a 'Mozart music playlist' video. While watching these videos, each subject held the pen-type EDA sensor, and their EDA responses were monitored and stored in a computer. Each subject also filled out pre-experiment and in-experiment surveys where they rated, respectively, their emotions associated with academic test-taking scenarios and their responses to emotion evoking videos that they just watched.

After these experiments were performed with 36 subjects (under Kansas State University IRB protocol #9864), the stored EDA data were processed through an EDA signal-processing app which extracts SCL and phasic EDA data from a raw EDA data set. Significant phasic EDA peaks were identified and recorded. These recorded data yielded peak time, rise time, phasic amplitude, onset time, and offset time parameters. Based on these data, statistical plots were created to choose one or more parameters to use for 'relaxed' versus 'stressed' classification and

detection. Eventually, the parameter 'phasic amplitude' was picked for stress detection. However, out of 5 different sets of EDA data, only 3 sets were used for stress detection. Those EDA data were collected from the 1st video (Mozart music), the 2nd video (parkour), and the 3rd video (jump-scaring). The EDA data from the 2nd and 3rd videos were combined together to become the 'stressed' data set. This is because the 'relaxed' data set from the 1st video is statistically different from the 2nd and 3rd data sets, whereas the EDA data from the 4th video (saying goodbye) and the 5th video (near-misses) did not show any statistical differences relative to the 1st EDA data set.

To build stress detection/classification models, normalized training data histograms were plotted against probability density functions (PDFs) for both the 'relaxed' and 'stressed' amplitudes, based on training/test ratios of 80/20 and 50/50. The data distributions were fitted with generalized extreme value (GEV) PDF models, which passed chi-squared goodness-of-fit tests when compared to the respective normalized histograms. The established GEV models for both the 'relaxed' and 'stressed' training data were then used to conduct likelihood ratio tests regarding whether to accept null or alternative hypotheses that related to relaxed versus stressed states, respectively. The likelihood ratio tests for the 80/20 and 50/50 scenarios offered outstanding performance. Additionally, similar likelihood ratio tests were conducted using a set of training data to establish GEV models based on individual subjects' EDA data (as opposed to randomly choosing data points from all subjects). The stress detection performance for this case offered relatively lower accuracy. However, results from both testing approaches validated the potential for this novel pen-type EDA sensing system to identify user stress levels, and this work will facilitate future research on psychological stress testing within academic environments.

B. Future Work

There are a number of ways to improve the pen-type EDA sensing system and the associated research endeavors. First, the PCB can be shrunk to fit inside the handgrip 'trainer' shell. If wireless technology, such as Bluetooth, is incorporated, the pen-type sensor can be lighter and free of wires, meaning the user can freely utilize the writing functionality of the device. This will allow future research to incorporate actual 'test taking' scenarios.

Second, algorithms will be needed to separate motion artifacts from EDA signals or at least minimize their contribution. The current EDA data are not corrupted by substantive motion artifacts because subjects are instructed not to move their hands during the data collection session. Since basic EDA signals evoked by various visual stimuli were successfully characterized by this research, motion-corrupted EDA signals are a sensible next step.

Third, 'superimposed' EDA signals can be studied. In the current effort, only one maximum peak for each onset & offset pair was acknowledged as a peak. However, 'superimposed' EDA peaks have psycho-physiological significance and should be studied.

Lastly, other various emotions including sadness, boredom, etc. can be studied in greater detail. In the current project, there was an attempt to differentiate 'sadness' from anxiety-based stress. However, the EDA data from the supposed sadness-evoking video ('saying goodbye') were not differentiable from the 'relaxed' data by the statistical method incorporated in this research.

References

1. Kaushik, A., et al., *Recent advances in cortisol sensing technologies for point-of-care application.* Biosensors and Bioelectronics, 2014. **53**: p. 499-512.

2. Sriramprakash, S., V.D. Prasanna, and O.V.R. Murthy, *Stress Detection in Working People.* Procedia Computer Science, 2017. **115**: p. 359-366.

3. Zhang, X., et al. *Recognition of public speaking anxiety on the recurrence quantification analysis of GSR signals*. in *2016 Sixth International Conference on Information Science and Technology (ICIST)*. 2016.

4. Brossaud, J., et al. *Urinary cortisol metabolites in corticotroph and adrenal tumours*. in *15th International & 14th European Congress of Endocrinology*. 2012. BioScientifica.

5. Arya, S., et al., *Antibody functionalized interdigitated μ-electrode (IDμE) based impedimetric cortisol biosensor.* The Analyst, 2010. **135**: p. 1941-6.

6. Russell, E., et al., *Hair cortisol as a biological marker of chronic stress: Current status, future directions and unanswered questions.* Psychoneuroendocrinology, 2012. **37**(5): p. 589-601.

7. Prunty, H., et al. *Sweat patch cortisol-a new screen for Cushing's syndrome*. in *British Endocrine Societies Joint Meeting*. 2004.

8. Levine, A., et al., *Measuring cortisol in human psychobiological studies.* Physiology & Behavior, 2007. **90**(1): p. 43-53.

9. Imaging, E.o.b.o.t.N.I.o.B., et al., *Improving healthcare accessibility through point-of-care technologies.* Clinical Chemistry, 2007. **53**(9): p. 1665-1675.

10. Sun, K., N. Ramgir, and S. Bhansali, *An immunoelectrochemical sensor for salivary cortisol measurement.* Sensors and Actuators B: Chemical, 2008. **133**(2): p. 533-537.

11. He, Z. and W. Jin, *Capillary electrophoretic enzyme immunoassay with electrochemical detection for thyroxine.* Analytical biochemistry, 2003. **313**(1): p. 34-40.

12. Chowdhury, A., et al., *Sensor Applications and Physiological Features in Drivers' Drowsiness Detection: A Review.* IEEE Sensors Journal, 2018. **18**(8): p. 3055-3067.

13. Villarejo, M.V., B.G. Zapirain, and A.M. Zorrilla, *A Stress Sensor Based on Galvanic Skin Response (GSR) Controlled by ZigBee.* Sensors, 2012. **12**(5): p. 6075.

14. Palanisamy, K., M. Murugappan, and S. Yaacob, *Multiple physiological signal-based human stress identification using non-linear classifiers.* Elektronika ir elektrotechnika, 2013. **19**(7): p. 80-85.

15. Varon, C., et al. *Removal of respiratory influences from heart rate during emotional stress*. in *2017 Computing in Cardiology (CinC)*. 2017.

16. Seoane, F., et al., *Wearable Biomedical Measurement Systems for Assessment of Mental Stress of Combatants in Real Time.* Sensors, 2014. **14**(4): p. 7120.

17. Pekrun, R., et al., *Measuring emotions in students' learning and performance: The Achievement Emotions Questionnaire (AEQ).* Contemporary Educational Psychology, 2011. **36**(1): p. 36-48.

18. Pekrun, R., *The control-value theory of achievement emotions: Assumptions, corollaries, and implications for educational research and practice.* Educational psychology review, 2006. **18**(4): p. 315-341.

19. Pekrun, R., A.J. Elliot, and M.A. Maier, *Achievement goals and discrete achievement emotions: A theoretical model and prospective test.* Journal of educational Psychology, 2006. **98**(3): p. 583.

20. Hu, Y., et al., *Neural control of sweat secretion: a review.* British Journal of Dermatology, 2018. **178**(6): p. 1246-1256.

21. Wysocki, A.B., *Skin anatomy, physiology, and pathophysiology.* The Nursing Clinics of North America, 1999. **34**(4): p. 777-97, v.

22. Elias, P.M., *Stratum corneum defensive functions: an integrated view.* Journal of General Internal Medicine, 2005. **20**(5): p. 183-200.

23. Sato, K., *The physiology, pharmacology, and biochemistry of the eccrine sweat gland*, in *Reviews of Physiology, Biochemistry and Pharmacology, Volume 79*. 1977, Springer. p. 51-131.

24. Sato, K. and F. Sato, *Individual variations in structure and function of human eccrine sweat gland.* American Journal of Physiology-Regulatory, Integrative and Comparative Physiology, 1983. **245**(2): p. R203-R208.

25. Shelley, W.B. and H.J. Hurley Jr, *The physiology of the human axillary apocrine sweat gland.* Journal of Investigative Dermatology, 1953. **20**(4): p. 285-297.

26. Malmivuo, J. and R. Plonsey, *Bioelectromagnetism. 27. The Electrodermal Response*. 1995. p. 428-434.

27. Boucsein, w., *Electrodermal Activity.* p. 66.

28. Sverre Grimnes, O.G.M., *Bioimpedance and Bioelectricity Basics.* p. 100.

29. Grimnes, S., *Psychogalvanic reflex and changes in electrical parameters of dry skin.* Medical and Biological Engineering and Computing, 1982. **20**(6): p. 734-740.

30. Yamamoto, T. and Y. Yamamoto, *Electrical properties of the epidermal stratum corneum.* Medical and biological engineering, 1976. **14**(2): p. 151-158.

31. Critchley, H.D., *Review: Electrodermal Responses: What Happens in the Brain.* The Neuroscientist, 2002. **8**(2): p. 132-142.

32. Yamamoto, Y. and T. Yamamoto, *Characteristics of skin admittance for dry electrodes and the measurement of skin moisturisation.* Medical and Biological Engineering and Computing, 1986. **24**(1): p. 71-77.

33. Braithwaite, J.J., et al., *A guide for analysing electrodermal activity (EDA) & skin conductance responses (SCRs) for psychological experiments.* Psychophysiology, 2013. **49**(1): p. 1017-1034.

34. *megatrue pencil pen handwriting aid*. Available from: https://oman.desertcart.com/products/40611416-megatrue-pencil-pen-ergonomics-handwriting-aid-grip-for-adult-and-kids-anti-skid.

35. Spangler, G., et al., *STUDENTS' EMOTIONS, PHYSIOLOGICAL REACTIONS, AND COPING IN ACADEMIC EXAMS.* Anxiety, Stress & Coping, 2002. **15**(4): p. 413.

36. Reinhard Pekrun, A.C.F., Thomas Goetz, & Raymond P. Perry, *Emotion in Education.* 2007: p. 20.

37. *Arduino nano*. 04/04/2020]; Available from: https://www.arduino.cc/en/pmwiki.php?n=Main/ArduinoBoardNano.

38. Olson, W.H., *Electrical safety*, in *Medical instrumentation: application and design*. 1978, Houghton Mifflin. p. 667-707.

39. Baek, H.J., et al., *Nonintrusive Biological Signal Monitoring in a Car to Evaluate a Driver's Stress and Health State.* Telemedicine and e-Health, 2009. **15**(2): p. 182-189.

40. *Adafruit ADS1115 16 BIT*. Available from: https://www.adafruit.com/product/1085.

41. *MegunoLink*. 04/04/2020]; Available from: https://www.megunolink.com/introduction/what-is-megunolink/.

42. Posada-Quintero, H.F., et al., *Power spectral density analysis of electrodermal activity for sympathetic function assessment.* Annals of biomedical engineering, 2016. **44**(10): p. 3124-3135.

43. Posada-Quintero, H.F., et al., *Time-varying analysis of electrodermal activity during exercise.* PloS one, 2018. **13**(6): p. e0198328-e0198328.

44. *Adafruit USB isolator*. 04/04/2020]; Available from: https://github.com/adafruit/Adafruit-USB-Isolator-PCB.

45. *Matlab App Designer*. [cited 04/04/2020; Available from: https://www.mathworks.com/products/matlab/app-designer.html.

46. Grigore, O., I. Gavat, and C. Grigore, *Psycho-Physiological Signal Processing and Algorithm for Adaptive Light Control*. 2008.

47. Response, G.S., *The complete pocket guide.* Imotions–Biometric Research, Simplified, 2017.

48. Gubner, J.A., *Probability and random processes for electrical and computer engineers*. 2006: cambridge university press.

49. Ferdinand van der Heijden, R.P.D., *Classification, parameter estimation and state estimation: an engineering approach using Matlab.* 2005: p. 23.

50. Anisimova, M. and O. Gascuel, *Approximate likelihood-ratio test for branches: a fast, accurate, and powerful alternative.* Systematic biology, 2006. **55**(4): p. 539-552.

51. Ramírez, J., et al., *Statistical voice activity detection using a multiple observation likelihood ratio test.* IEEE Signal Processing Letters, 2005. **12**(10): p. 689-692.

Appendix A - Informed consent form

This appendix contains the informed consent form that every experiment participant read and signed. The document addresses a brief description of the research, the procedures, and the possible risks.

INFORMED CONSENT FORM – ELECTRODERMAL ACTIVITY (EDA) SENSING STUDY

PROJECT TITLE: Pen-Type Electrodermal Activity (EDA) Sensing Device for Academic Test Anxiety Monitoring

APPROVAL DATE: **09/06/2019**
EXPIRATION DATE: **09/06/2022**

PRINCIPAL INVESTIGATOR

Steve Warren, Ph.D., Kansas State University (KSU), Electrical & Computer Engineering (ECE), 3018 Engineering Hall, Kansas State University, Manhattan, KS 66506, swarren@ksu.edu, 785-532-4644

CO-INVESTIGATOR(S)

Taehee Lee, KSU ECE, taeheelee@ksu.edu, 785-532-5600

CONTACT FOR ANY PROBLEMS/QUESTIONS

Taehee Lee, KSU ECE, taeheelee@ksu.edu, 785-532-5600

IRB CHAIR/OFFICE CONTACT INFORMATION

- Rick Scheidt, Chair, Committee on Research Involving Human Subjects
- Heath Ritter, Research Compliance Manager
- Cheryl Doerr, Associate Vice President for Research Compliance,

University Research Compliance Office, 203 Fairchild Hall, Kansas State University, Manhattan, KS 66506, (785) 532-3224

PROJECT SPONSOR: N/A

RESEARCH PURPOSE: The purpose of this effort is to gage the ability of a lightweight, pen-type device to acquire mood-related data from a person's hand while they participate in an emotion-evoking experience.

PROCEDURES OR METHODS TO BE USED: At the beginning of the session, you will be asked to complete a short survey regarding emotions that you typically associate with academic test taking. The researcher will then ask you to hold a pen-type sensing device while you watch a series of emotive videos. Prior to this video session, the researcher will also attach a set of electrodes that allow additional physiological information to be gathered from you as you watch the videos. This video material will be presented in a predetermined sequence, and the researcher will pause periodically to ask you about your response to that content. The entire session will be videotaped and last about 30 minutes. Data gathered by the pen-type device and the electrodes will be stored in a computer. At the conclusion of the session, you will receive a debriefing statement that affirms the purpose of the research and describes the data that were gathered.

ALTERNATIVE PROCEDURES OR TREATMENTS, IF ANY, THAT MIGHT BE ADVANTAGEOUS TO SUBJECT: N/A.

LENGTH OF STUDY: This study and the follow-on analyses will occur primarily during the Fall 2019 academic semester.

RISKS OR DISCOMFORTS ANTICIPATED: The pen-type device and electrodes are completely safe – they pose no measurable risk to the subject or the researcher. It is possible, though unlikely, that you may experience emotional distress from a given video, even though this video material has been vetted to avoid extreme content. If this is the case, please describe your feelings to the researcher, and the two of you can decide whether it is sensible to continue.

BENEFITS ANTICIPATED: Test anxiety is a substantive issue for many college students. This work is intended to develop tools that can help to quantify academic stress and anxiety without interfering with the test taking process itself. The eventual goal is to better understand optimal means to present assessment material to the student while minimizing their emotional response to the process. However, there will not be any direct benefits, such as monetary prizes or gifts, to the participants.

EXTENT OF CONFIDENTIALITY: All session data will be stored on a password-protected network drive managed by the KSU College of Engineering and/or password-protected computers managed by the PI and the graduate student that conduct this work. Signed consent forms and physical session products will be stored in a locked file cabinet. To maintain your confidentiality, you will be assigned a unique number that will then be used to identify you thereafter; you will not be completely anonymous from the perspective of the researcher.

FURTHER USE OF EXPERIMENAL DATA: All of the sensor data acquired by the researcher will be de-identified, meaning that your identity will not be associated with these data. Because these data may prove useful, for example, as comparative data for follow-on efforts, it is possible that these data might be used for future research studies or may be distributed to another investigator for future research studies without additional informed consent. In any case, your identity will remain confidential and will not be made available to these other researchers. If these data result in commercial profit (which is unanticipated), subjects will not share in that profit. Clinically relevant research results will not be provided to subjects.

TERMS OF PARTICIPATION: I understand that this project involves research and that my participation is voluntary. I also understand that if I decide to participate, I may withdraw my consent and stop participation at any time without explanation, penalty, or loss of benefits to which I may otherwise be entitled.

M**y signature below indicates that I have read and understand this consent form, and I agree to participate in this study under the terms described.**

Participant Signature: _____ **Date:** _____

Witness to Signature:
(Project Staff) _____ **Date:** _____

Appendix B - Experiment surveys

The pre- and in-experiment surveys follow. The pre-experiment survey was given to every participant prior to data collection. A portion of the in-experiment survey was offered after each emotion-evoking video.

Pre-Experiment Survey

Subject Name: _____; **Subject Number (Assigned): _____**

Email Address: _____; **Phone Number: _____**

Sex: _____; Age: _____;

Based on your past experiences, what positive or negative emotions do you associate with the process of 'taking an academic exam?' Circle all that apply.

Happiness Relaxation Pride Sadness Anxiety Hopelessness Anger Shame Boredom

For each emotion that you identified above, rate that single emotion on a scale of 1 to 10 in the context of a typical exam experience, where

1 = a <u>minimal</u> sense of emotion and 10 = an <u>extreme</u> sense of emotion

Happiness:	**1**	**2**	**3**	**4**	**5**	**6**	**7**	**8**	**9**	**10**
Relaxation:	**1**	**2**	**3**	**4**	**5**	**6**	**7**	**8**	**9**	**10**
Pride:	**1**	**2**	**3**	**4**	**5**	**6**	**7**	**8**	**9**	**10**
Sadness:	**1**	**2**	**3**	**4**	**5**	**6**	**7**	**8**	**9**	**10**
Anxiety:	**1**	**2**	**3**	**4**	**5**	**6**	**7**	**8**	**9**	**10**
Hopelessness:	**1**	**2**	**3**	**4**	**5**	**6**	**7**	**8**	**9**	**10**
Anger:	**1**	**2**	**3**	**4**	**5**	**6**	**7**	**8**	**9**	**10**
Shame:	**1**	**2**	**3**	**4**	**5**	**6**	**7**	**8**	**9**	**10**
Boredom:	**1**	**2**	**3**	**4**	**5**	**6**	**7**	**8**	**9**	**10**

In-Experiment Survey

Video 1 – Mozart Music Video

How relaxed are you after listening to this music, where 1 = "not relaxed at all" and 10 = "extremely relaxed?"

1 2 3 4 5 6 7 8 9 10

Video 2 – Parkour Video

How nervous did this video make you feel, where 1 = "not at all" and "10 = extremely nervous?"

1 2 3 4 5 6 7 8 9 10

Video 3 – Jump Scaring Video

How startled were you during this video, where "1 = not at all" and "10 = extremely … I was scared every time?"

1 2 3 4 5 6 7 8 9 10

Did you physically move while watching this video?

Yes No

Video 4 –Saying Goodbye Video

How sad did this video make you feel, where "1 = not at all" and "10 = extremely … I almost cried?"

1 2 3 4 5 6 7 8 9 10

Video 5 – Near Miss Video

How stressed were you while watching this video, where "1 = not at all" and "10 = extremely?"

1 2 3 4 5 6 7 8 9 10

Appendix C - Research protocol

This appendix contains the research protocol. The expected duration of a session is about 30 minutes. The necessary research materials are first listed, and then the data collection procedures are numbered and explained step by step.

Electrodermal Activity (EDA) Measurement Protocol

Expected duration: 30 minutes

Materials

- Pen-type EDA sensing device
- Noise cancelling headphones
- Video camera (e.g., smart phone camera)
- Data acquisition laptop & video-playing screen (iPad)
- Emotion-evoking videos (Mozart music, parkour video, jump-scaring video, saying goodbye video, near miss video)
- The research video compilation that is used in this project can be found in the URL written below:

https://ksuemailprod-my.sharepoint.com/:v:/g/personal/taeheelee_ksu_edu/EQFfK6PNlJRCnIw79lJnzVoB0eMosNDvvB72d7KSJdFz8w?e=xTBZcs

1) Pre-Experiment Survey (5 min)

Ask the subject to respond to the survey items prior to the experiment (see *EDA Survey.docx*)

2) Data Acquisition Setup

- Employ MegunoLink for real-time plotting (two separate Arduino signals can be plotted simultaneously)

- Use the subject's right thumb and index finger to gather EDA data

- Prepare the laptop computer and smart phone for data and video logging, respectively

3) EDA Data Acquisition Protocol (~20 min)

The following is the overall protocol for EDA data collection. The instructions are the same for each video, but the post-video survey questions differ. Written instructions are superimposed on each video so that the subject knows what to do as they watch.

1. The subject completes the pre-experiment survey.
2. The subject sits next to the researcher so that the researcher can see what's playing on the screen.
3. The researcher shows the subject how to properly grip the pen/pencil trainer so as to make proper contact with the EDA electrodes.
4. The researcher briefly explains the video display process and the times when the subject needs to grip the EDA device.
5. The researcher initiates data logging and video-camera acquisition.
6. After the explanation, the researcher plays the first video (20 seconds of instruction followed by 2~4 min of video content). When the video starts, the researcher records the timestamps on the data acquisition and camera equipment. If any subject movement occurs, the researcher also takes a note of it. After the video, the researcher pauses the data acquisition equipment and camera so that the subject has time to answer the survey question for the video. After the subject answers the survey question, the researcher saves the recorded EDA data '.csv' files via MegunoLink.
7. Items 6 is repeated for the other videos employed during the session.

Appendix D - Extra Experimental Data

Appendix D contains extra experimental data. Boxplots of EDA phasic data with moving average filter windows of widths 81, 141, and 201 are attached. Unstandardized phasic EDA data are attached as well.

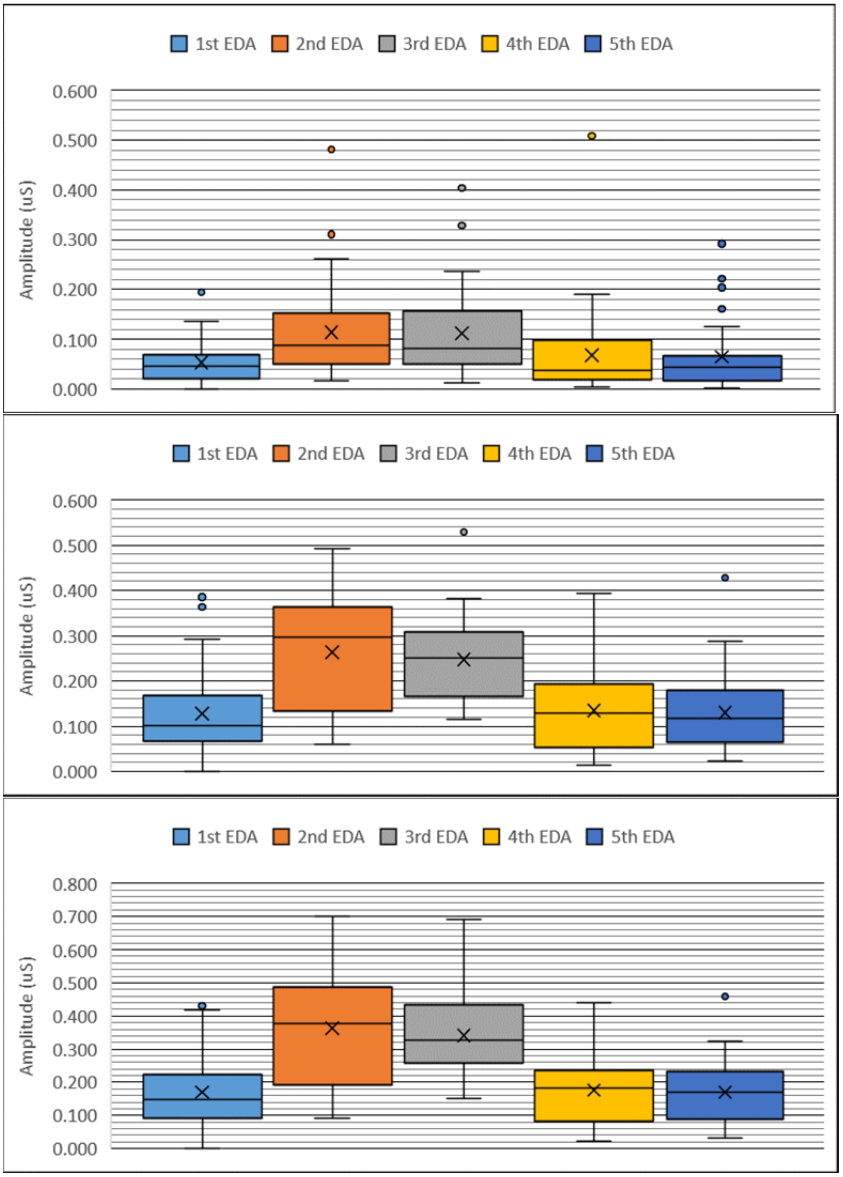

Figure 36. Boxplots of EDA responses for each video with an 81-wide moving average filter window: unstandardized (top), standardized (middle), and standardized with a three-maxima average (bottom).

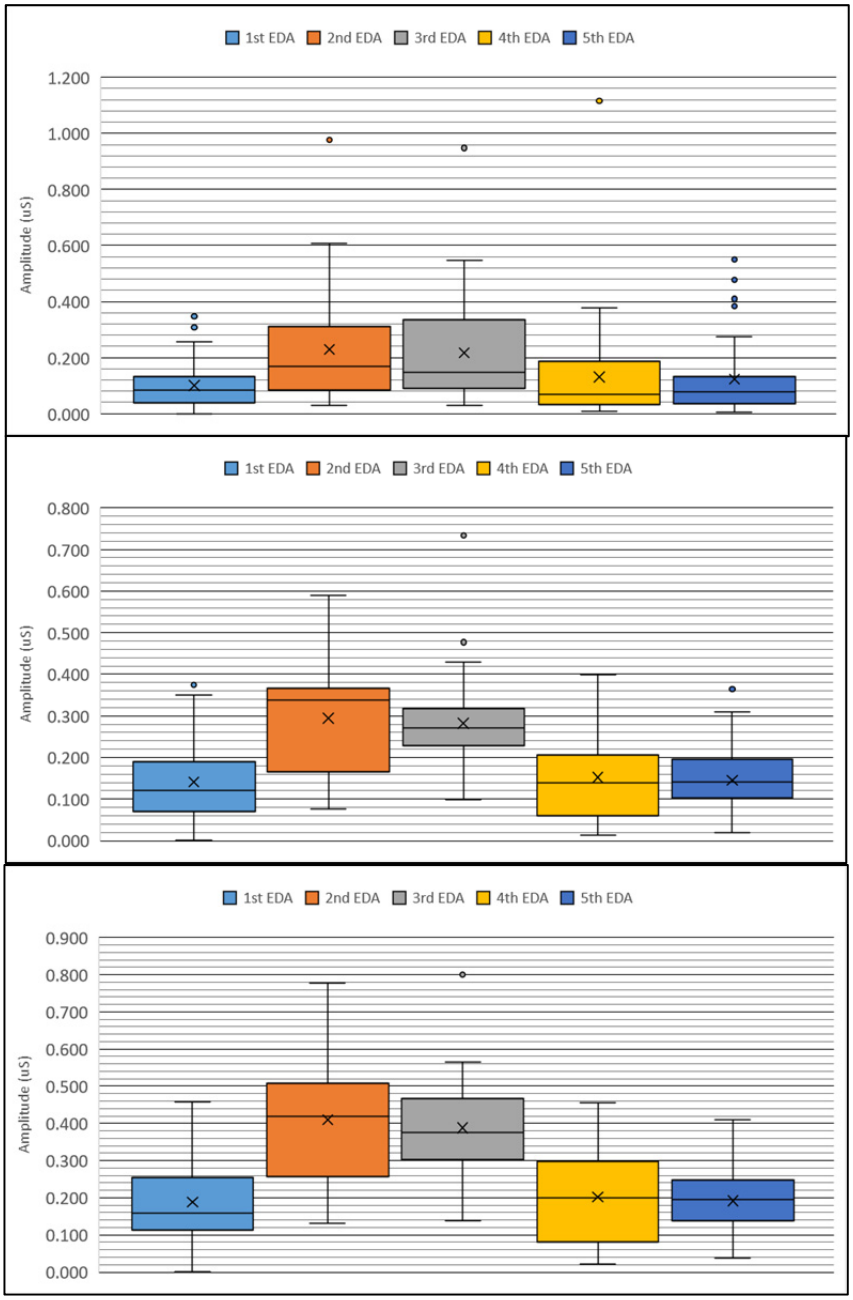

Figure 37. Boxplots of EDA responses for each video with a 141-wide moving average filter window: unstandardized (top), standardized (middle), and standardized with a three-maxima average (bottom).

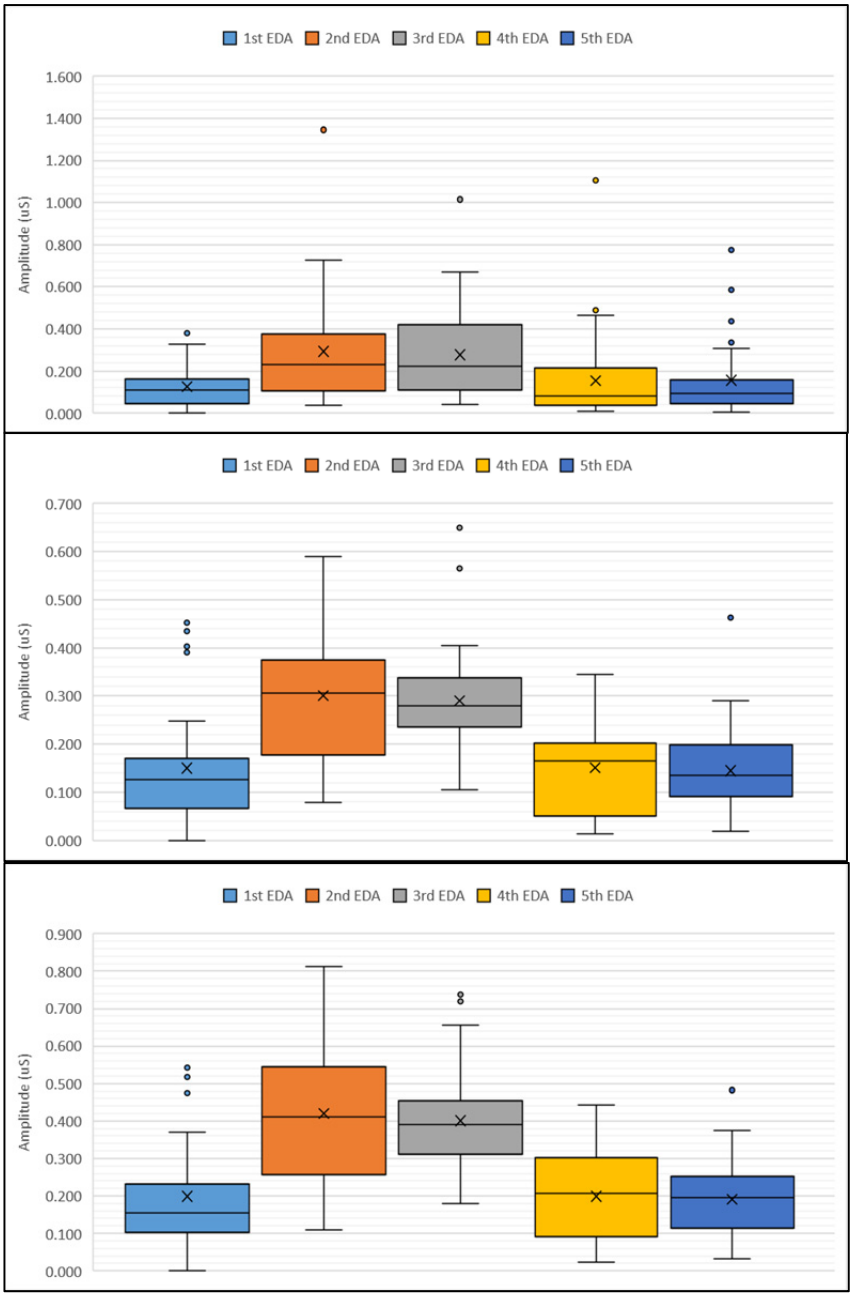

Figure 38. Boxplots of EDA responses for each video with a 201-wide moving average filter window: unstandardized (top), standardized (middle), and standardized with three-maxima average (bottom).

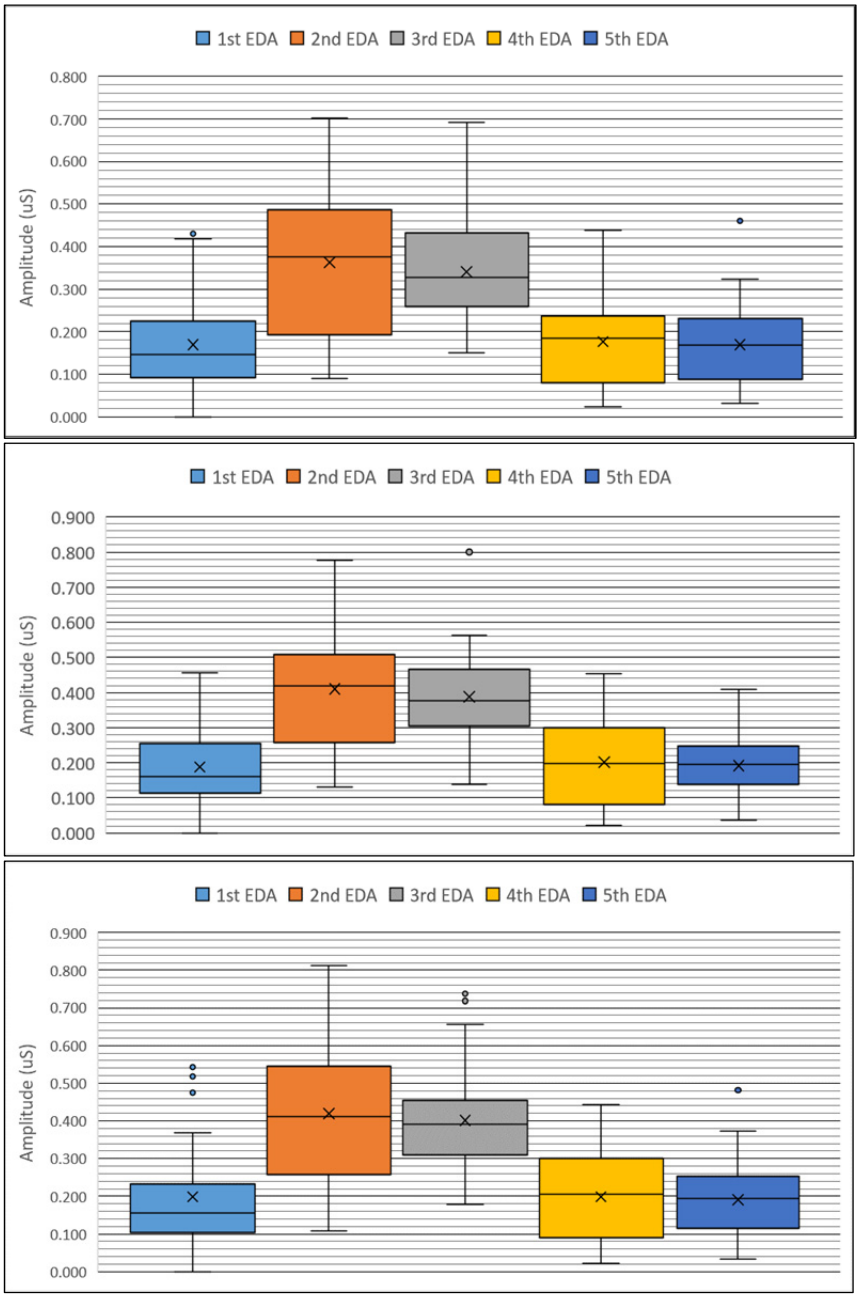

Figure 39. Boxplots of EDA responses for each video with the three-maxima average standardization. Average filter window width: 81 (top), 141 (middle), and 201 (bottom).

Appendix E - Extra Stress Detection Data

The first section of this appendix contains model parameters and Z values for the GEV models that were fitted to different test data. The second section contains all likelihood ratios calculated when varying the 'training' to 'test' ratios.

	Test 1	*Test 2*	*Test 3*	*Test 4*	*Test 5*	*Test 6*	*Test 7*
ξ_relaxed	5.84E-01	5.61E-01	5.48E-01	6.05E-01	4.87E-01	5.92E-01	5.60E-01
σ_relaxed	8.37E-02	8.68E-02	8.00E-02	7.81E-02	8.22E-02	7.77E-02	8.93E-02
μ_relaxed	7.41E-02	7.99E-02	7.41E-02	7.22E-02	7.95E-02	7.21E-02	8.22E-02
ξ_stressed	3.86E-01	3.49E-01	3.53E-01	3.47E-01	3.06E-01	2.98E-01	3.70E-01
σ_stressed	2.04E-01	2.06E-01	1.97E-01	1.95E-01	2.17E-01	2.06E-01	1.97E-01
μ_stressed	2.13E-01	2.22E-01	2.14E-01	2.09E-01	2.36E-01	2.20E-01	2.13E-01
Zx	4.52E+00	6.48E+00	5.48E+00	6.90E+00	9.49E+00	6.68E+00	6.13E+00
Zy	3.79E+00	4.22E+00	4.75E+00	2.69E+00	3.73E+00	3.80E+00	3.89E+00

	Test 8	*Test 9*	*Test 10*	*Test 11*	*Test 12*	*Test 13*	*Test 14*	*Test 15*
ξ_relaxed	5.24E-01	7.04E-01	5.73E-01	5.49E-01	5.66E-01	5.70E-01	5.91E-01	6.48E-01
σ_relaxed	7.92E-02	7.20E-02	7.64E-02	8.15E-02	8.54E-02	7.61E-02	8.07E-02	7.64E-02
μ_relaxed	7.60E-02	6.18E-02	6.92E-02	7.38E-02	7.81E-02	7.02E-02	7.32E-02	6.64E-02
ξ_stressed	3.11E-01	3.41E-01	3.84E-01	3.52E-01	3.31E-01	3.93E-01	3.94E-01	3.42E-01
σ_stressed	2.01E-01	1.95E-01	2.08E-01	2.07E-01	1.98E-01	1.92E-01	1.97E-01	1.99E-01
μ_stressed	2.20E-01	2.15E-01	2.21E-01	2.20E-01	2.22E-01	2.03E-01	2.09E-01	2.15E-01
Zx	8.89E+00	5.64E+00	7.40E+00	7.69E+00	6.57E+00	7.51E+00	6.81E+00	5.90E+00
Zy	4.39E+00	3.68E+00	3.60E+00	4.15E+00	2.93E+00	3.86E+00	3.35E+00	4.84E+00

Table 10. Estimated GEV model parameters and Z values for 15 different data sets (50/50).

	Test 1	*Test 2*	*Test 3*	*Test 4*	*Test 5*	*Test 6*	*Test 7*
likelihood_relax_1	9.12E-03	3.50E-06	6.52E-04	1.81E-08	1.46E-08	1.19E-06	1.75E-07
likelihood_relax_2	2.81E-05	3.71E-07	3.61E-03	3.77E-03	3.26E-03	5.82E-07	1.54E-04
likelihood_relax_3	1.40E-06	2.74E-01	4.83E-08	1.81E-04	3.01E-08	5.01E-04	4.11E-11
likelihood_relax_4	3.67E-10	1.91E-06	2.12E-06	6.05E-04	1.47E-08	7.61E-10	1.06E-05
likelihood_relax_5	4.47E-07	1.57E-10	2.00E-04	3.43E-05	6.21E-05	5.81E-05	1.68E-03

	Test 8	*Test 9*	*Test 10*	*Test 11*	*Test 12*	*Test 13*	*Test 14*	*Test 15*
likelihood_relax_1	1.35E-06	3.03E-09	5.84E-06	1.54E-11	4.75E-06	2.28E-06	1.63E-04	5.51E-07
likelihood_relax_2	6.36E-05	5.87E-09	2.21E-06	4.56E-09	4.21E-09	2.23E-08	5.29E-07	1.83E-04
likelihood_relax_3	1.14E-08	3.40E-06	5.74E-04	6.90E-03	7.95E-06	5.30E-04	9.12E-07	1.60E-03
likelihood_relax_4	3.86E-08	2.51E-08	6.19E-08	6.00E-05	2.67E-07	2.31E-04	4.16E-07	3.67E-04
likelihood_relax_5	5.40E-02	9.17E-07	2.92E-05	3.94E-07	5.36E-10	8.38E-07	8.79E-11	4.19E-09

Table 11. Table of likelihood ratios for the 'relaxed' test data sets using an 80/20 ratio.

	Test 1	*Test 2*	*Test 3*	*Test 4*	*Test 5*	*Test 6*	*Test 7*
likelihood_stress_1	1.80E+05	2.17E+02	2.91E+07	5.28E+06	1.80E+03	6.46E+03	4.68E+04
likelihood_stress_2	5.94E+04	3.32E+03	1.68E+03	2.73E+05	4.30E+07	3.40E+01	2.52E+06
likelihood_stress_3	2.31E+02	2.92E+05	2.87E+06	1.57E+06	5.08E+05	2.17E+06	1.03E+02
likelihood_stress_4	1.38E+08	2.02E+06	1.90E+04	7.21E+05	1.49E+02	3.52E+07	1.14E+06
likelihood_stress_5	1.96E+02	8.61E+02	2.98E+07	7.81E+04	1.29E+06	5.62E+06	3.24E+08

	Test 8	*Test 9*	*Test 10*	*Test 11*	*Test 12*	*Test 13*	*Test 14*	*Test 15*
likelihood_stress_1	3.43E+04	5.88E+04	4.64E+06	3.38E+05	1.62E+05	6.98E+00	5.90E-01	1.21E+07
likelihood_stress_2	9.71E+04	5.00E+04	1.53E+05	1.64E+03	2.25E+06	4.31E+06	7.92E-02	3.94E+02
likelihood_stress_3	1.34E+02	4.36E+02	4.19E+04	1.04E+05	2.56E+02	3.55E+06	7.11E-02	3.75E+07
likelihood_stress_4	2.35E+05	1.72E+02	5.43E+07	4.17E+03	7.98E+06	7.24E+04	3.27E-01	2.84E+01
likelihood_stress_5	4.30E+04	5.38E+04	1.02E+04	2.44E+05	1.06E+05	4.93E+07	2.01E-01	6.36E+09

Table 12. Table of likelihood ratios for the 'stressed' test data sets using an 80/20 ratio.

	Test 1	*Test 2*	*Test 3*	*Test 4*	*Test 5*	*Test 6*	*Test 7*
likelihood_relax_1	4.61E-03	8.36E-09	5.24E-06	4.79E-03	5.29E-06	5.32E-05	9.60E-09
likelihood_relax_2	7.60E-04	1.56E-04	1.29E-03	2.27E-06	1.89E-04	3.09E-07	6.08E-06
likelihood_relax_3	3.38E-06	3.66E-05	5.98E-06	8.32E-07	1.44E-07	5.54E-09	1.46E-07
likelihood_relax_4	2.38E-05	7.44E-06	1.69E-06	1.64E-05	2.72E-07	2.71E-07	1.79E-09
likelihood_relax_5	6.46E-07	3.48E-06	1.33E-06	6.88E-03	2.98E-03	7.05E-07	4.22E-10
likelihood_relax_6	8.64E-06	9.83E-07	7.46E-09	1.27E-02	9.01E-07	8.27E-08	1.63E-07
likelihood_relax_7	1.09E-04	1.46E-07	3.01E-03	3.06E-08	1.03E-08	1.72E-05	3.12E-07
likelihood_relax_8	1.59E-09	1.24E-05	4.87E-11	1.07E-06	3.07E-06	2.89E-05	2.34E-04
likelihood_relax_9	2.87E-03	2.39E-07	1.51E-07	1.38E-05	4.77E-06	2.48E-06	4.30E-03
likelihood_relax_10	2.71E-02	2.20E-08	3.13E-05	3.20E-01	1.45E-09	1.97E-08	3.10E-09
likelihood_relax_11	2.54E-05	1.29E-11	5.92E-10	3.67E-04	4.61E-09	1.58E-05	1.62E-05
likelihood_relax_12	7.49E-08	9.32E-07	7.31E-07	6.77E-03	9.59E-07	7.40E-08	1.66E-06
likelihood_relax_13	3.52E-05	7.26E-08	6.08E-05	4.44E-07	1.12E-08	9.17E-08	1.14E-09

	Test 8	*Test 9*	*Test 10*	*Test 11*	*Test 12*	*Test 13*	*Test 14*	*Test 15*
likelihood_relax_1	1.85E-07	3.93E+00	6.54E-10	7.63E-07	6.41E-08	2.48E+00	2.23E-04	4.76E-09
likelihood_relax_2	8.86E-06	3.38E-07	1.43E-05	1.32E-07	1.18E-05	5.05E-04	7.31E-07	5.40E-05
likelihood_relax_3	8.90E-07	3.10E-08	4.35E-07	2.44E-06	2.14E-08	1.82E-04	4.82E-06	4.07E-05
likelihood_relax_4	2.00E-07	1.09E-08	1.06E-05	6.01E-07	9.36E-06	6.19E-08	1.83E-05	7.49E-06
likelihood_relax_5	3.54E-07	2.03E-06	3.85E-07	1.98E-06	2.33E-07	6.50E-03	6.39E-04	4.33E-04
likelihood_relax_6	4.38E-06	1.43E-04	3.83E-04	8.57E-07	2.35E-06	2.04E-05	3.63E-03	1.72E-06
likelihood_relax_7	2.26E-07	2.90E-05	5.70E-07	1.55E-09	6.25E-07	4.05E-07	1.36E-06	1.90E-04
likelihood_relax_8	6.62E-05	1.69E-02	7.70E-07	5.88E-04	7.79E-08	6.63E-07	1.01E-07	1.64E-05
likelihood_relax_9	4.47E-08	4.66E+00	1.08E-03	3.61E-10	6.61E-09	1.73E-04	8.20E-12	1.39E-04
likelihood_relax_10	1.08E-07	4.50E-07	5.38E-06	1.01E-11	5.55E-04	5.81E-02	4.09E-04	9.05E-07
likelihood_relax_11	1.28E-09	4.60E-06	4.06E-05	1.21E-05	1.61E-04	7.27E-03	3.74E-08	1.25E-02
likelihood_relax_12	2.13E-08	2.86E-05	1.36E-03	8.08E-05	3.72E-08	2.84E-06	1.55E-06	9.36E-08
likelihood_relax_13	6.53E-06	5.95E-04	4.87E-10	2.91E-04	1.13E-05	1.59E-03	9.83E-11	1.96E-07

Table 13. Table of likelihood ratios for the 'relaxed' test data sets using a 50/50 ratio.

	Test 1	*Test 2*	*Test 3*	*Test 4*	*Test 5*	*Test 6*	*Test 7*
likelihood_stress_1	1.97E+03	3.03E+05	8.80E+05	2.88E-03	1.62E+06	5.96E+05	2.48E+06
likelihood_stress_2	2.09E+07	5.34E+00	1.49E+04	1.50E+07	1.48E+05	3.08E+03	1.43E+03
likelihood_stress_3	1.10E+03	2.31E+01	1.41E+06	7.08E+04	3.17E+05	2.48E+03	2.29E+05
likelihood_stress_4	1.32E+05	1.83E+04	6.30E+06	1.47E+05	7.76E+06	8.00E+04	7.76E+03
likelihood_stress_5	1.25E+04	3.51E+04	1.09E+05	1.08E+04	2.38E+02	9.96E+01	4.63E+05
likelihood_stress_6	2.48E+04	3.19E+03	3.16E+04	1.33E+06	2.71E+02	2.71E+04	1.63E+05
likelihood_stress_7	8.62E+01	8.39E+07	4.74E+06	1.92E+04	9.66E+03	2.43E+04	1.37E+01
likelihood_stress_8	1.54E+07	1.39E+07	1.67E+05	1.33E+07	7.97E+06	7.04E+07	1.07E+05
likelihood_stress_9	1.67E+03	3.40E+05	3.47E+05	8.72E+06	5.58E+07	5.34E+03	1.33E+05
likelihood_stress_10	3.65E+09	7.37E+02	6.10E+03	7.84E+05	6.46E+06	2.90E+07	9.73E+02
likelihood_stress_11	2.66E+01	2.65E+04	4.00E+05	1.62E+05	1.13E+08	5.16E+07	1.26E+03
likelihood_stress_12	3.83E+07	4.31E+05	6.73E+03	1.82E+06	1.49E+03	2.98E+03	4.75E+06
likelihood_stress_13	2.68E+09	7.27E+00	6.50E+04	4.91E+04	1.21E+03	4.81E+03	9.64E+04

	Test 8	*Test 9*	*Test 10*	*Test 11*	*Test 12*	*Test 13*	*Test 14*	*Test 15*
likelihood_relax_1	2.97E+06	8.73E+02	1.30E+05	3.52E+00	7.59E+05	1.40E+04	2.12E+07	7.05E+03
likelihood_relax_2	3.35E+06	8.01E+01	2.75E+05	3.10E+03	4.02E+03	4.44E+05	3.20E+06	1.30E+02
likelihood_relax_3	2.29E+06	1.91E+07	9.78E+03	9.98E+04	3.83E+04	5.04E+07	1.98E+03	4.46E+05
likelihood_relax_4	4.55E+02	1.46E+06	1.57E+04	9.92E+06	1.91E+04	1.81E+06	1.64E+07	9.19E+07
likelihood_relax_5	5.12E+03	4.47E+05	1.71E+07	3.32E+02	1.75E+02	3.56E+06	6.19E+00	3.91E+04
likelihood_relax_6	2.39E+06	2.28E+04	8.17E+01	1.19E+03	1.09E+03	4.67E+04	8.43E+05	1.65E+07
likelihood_relax_7	1.32E+07	1.10E+05	1.46E+04	3.87E+06	2.35E+05	1.43E+09	4.04E+10	3.15E+03
likelihood_relax_8	8.00E+02	4.48E+08	3.55E+04	6.74E+05	2.25E+03	2.34E+06	2.12E+03	6.81E+09
likelihood_relax_9	6.61E+03	7.79E+07	7.68E+01	2.81E+09	2.31E+01	2.59E+05	1.55E+06	2.22E+04
likelihood_relax_10	3.76E+06	1.23E+03	4.22E+05	3.56E+09	3.66E-01	3.86E+06	2.56E+07	3.34E+05
likelihood_relax_11	1.46E+04	1.72E+08	4.76E+04	3.80E+05	1.89E+00	3.63E+06	7.82E+03	8.62E+04
likelihood_relax_12	1.34E+05	1.81E+06	8.77E+09	1.20E-02	2.97E+05	3.54E+07	3.20E+05	3.11E+05
likelihood_relax_13	8.40E+02	3.37E+08	2.22E+03	3.59E+03	2.61E+04	5.43E+07	8.89E+04	2.69E+06

Table 14. Table of likelihood ratios for the 'stressed' test data sets using a 50/50 ratio.

	Subject 1	*Subject 2*	*Subject 3*	*Subject 4*	*Subject 5*	*Subject 6*	*Subject 7*	*Subject 8*	*Subject 9*	*Subject 10*
relax_1	1.9E-13	1.1E-19	4.9E-06	2.9E-14	8.9E-06	7.7E-05	8.0E-02	1.3E-03	1.7E+00	1.9E-12
stress_1	2.9E+06	1.8E+01	1.6E-02	1.6E-01	5.2E+08	4.0E-05	9.1E+07	6.8E+00	1.2E-05	2.8E+06
stress_2	1.0E+02	5.4E+00	2.9E+02	1.6E+04	9.7E+01	2.2E-01	1.4E+03	1.7E+05	3.3E+01	2.5E+02

	Subject 11	*Subject 12*	*Subject 13*	*Subject 14*	*Subject 15*	*Subject 16*	*Subject 17*	*Subject 18*	*Subject 19*	*Subject 20*
relax_1	8.7E-10	9.4E-05	1.9E-02	2.9E-04	6.5E+01	2.6E-03	1.6E-03	1.1E-01	5.1E-15	1.2E-05
stress_1	6.0E+05	3.9E+03	3.3E+08	4.7E+07	1.1E+05	8.9E+06	1.6E+05	1.7E-04	1.1E+06	7.4E+06
stress_2	1.7E+03	2.9E-01	5.0E+01	7.6E+01	1.9E+00	8.7E+03	2.8E-03	1.9E+02	1.2E+03	2.2E+00

Table 15. Table of likelihood ratios for the 'relaxed', 'stressed 1' and 'stressed 2' test data sets.

Appendix F - PCB Circuit Schematic

The circuit schematic for the Adafruit USB isolator PCB is laid out below.

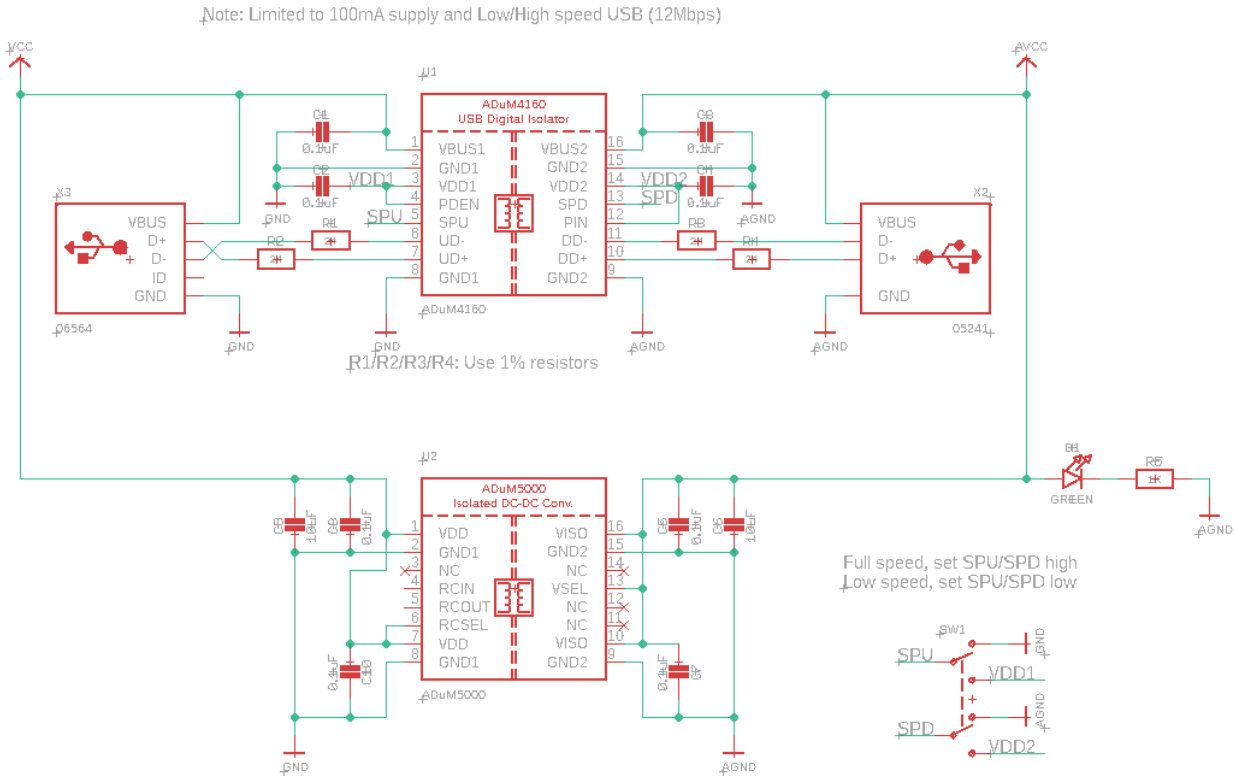

Figure 40. Adafruit USB isolator circuit schematic [44].